ABSTRACT

COMPARISON OF ADAPTIVE RADAR ALGORITHMS: TRANSFORMED SMI, EIGENCANCELER, AND SMI

by
Chaitanya H. Kathiari

Advanced airborne radars must perform target detection in the presence of interference and heavy clutter. In many applications, the practical usefulness of adaptive arrays is limited by their convergence rate. In this paper, we first analyze the performance of the SMI method. Then, two other methods, the transformed SMI and the eigencanceler, both based on the principle component inversion (PCI) technique, are described and analyzed by simulation. It is shown by simulation based comparison that the transformed SMI and the Eigencanceler outperform the SMI method. It is also shown that the transformed SMI and the eigencanceler has higher convergence rate in terms of output signal-to-noise ratio than the SMI, specially for short data record sizes. It is concluded that the transformed SMI and the eigencanceler are good alternatives to the SMI method when data set available is small.

COMPARISON OF ADAPTIVE RADAR ALGORITHMS:
TRANSFORMED SMI, EIGENCANCELER, AND SMI

by
Chaitanya H. Kathiari

A Thesis
Submitted to the Faculty of
New Jersey Institute of Technology
in Partial Fulfillment of the Requirements for the Degree of
Master of Science in Electrical Engineering

Department of Electrical and Computer Engineering

January 1996

Blank Page

APPROVAL PAGE

COMPARISON OF ADAPTIVE RADAR ALGORITHMS: TRANSFORMED SMI, EIGENCANCELER, AND SMI

Chaitanya H. Kathiari

Dr. Alexander Haimovich, Thesis Adviser   Date
Associate Professor of Electrical Engineering, NJIT

Dr. Yeheskel Bar-Ness   Date
Director of the Center for Communications and Signal Processing
Distinguished Professor of Electrical Engineering, NJIT

Dr. Yun-Qing Shi   Date
Assistant Professor of Electrical Engineering, NJIT

BIOGRAPHICAL SKETCH

Author: Chaitanya H. Kathiari

Degree: Master of Science in Electrical Engineering

Date: January 1996

Undergraduate and Graduate Education:

- Master of Science in Electrical Engineering
  New Jersey Institute of Technology, Newark, NJ, 1996

- Bachelor of Science in Electrical Engineering
  New Jersey Institute of Technology, Newark, NJ, 1994

Major: Electrical Engineering

This Thesis is dedicated to
My Parents

ACKNOWLEDGMENT

The author wishes to express his sincere gratitude to his supervisor, Dr. Alexander Haimovich, for his guidance and moral support throughout this research.

Special thanks to Dr. Bar-Ness and Dr. Shi for serving as members of the committee.

The author also wishes to thank Xiao Cheng Wu for suggestions and help during programming.

And finally, the author wishes to thank Dr. A. Haimovich again for being an adviser in true sense.

TABLE OF CONTENT

LIST OF FIGURES

LIST OF FIGURES
(Continued)

CHAPTER 1

INTRODUCTION

Adaptive array processors are currently of interest for a variety of applications in radar, communications, and sonar. They received much attention in the literature [1], [2] due to their capability for automatically cancelling interferences while preserving the desired signal. In an adaptive array, the complex envelope obtained from each element of the receiving antenna is sampled and multiplied by a complex weight component. Superposition of these weighted outputs is used to form a receiving beam with nulls steered onto interferences. The complex weights of this spatial filter are controlled by a processor or adaptive loops. In radar such adaptive systems are designed to maximize the probability of signal detection, which is equivalent in the Gaussian interference case to the maximization of the signal-to-noise ratio (SNR) at the output of the filter. In practical applications, besides maximization of probability of detection, we are concerned with the convergence speed of the adaptive beamformer since it determines the ability of an adaptive beamformer to adapt itself to rapidly changing interference environment.

Many techniques have been developed for adaptive beamforming in the literature over the years [3], [4]. Widrow [5] and associates at Stanford University were among the first who started research in the adaptive array field. Besides [5], Applebaum's [6] theory of adaptive arrays which maximizes SNR is considered the benchmark in this area. The number of weight adaptation algorithms has been growing rapidly over the years [7-17].

Published work in this field could be categorized in three major subtypes. We will name them as Type I, Type II, and Type III in this paper. Following paragraphs describe each subtype and provide examples of published work that falls into particular subtype.

Type I includes papers which introduce new algorithms. In [7], Brennan and Reed introduced the theory of adaptive radar. They utilized the method of steepest ascent to recursively update the weight vector such that the output signal-to-noise ratio is maximized. When the array correlation matrix is not known, it can be approximated from the data, as proposed in [8]. Using this estimated correlation matrix, the algorithm to calculate weight vector is developed in [8] which is known as the sample matrix inversion (SMI). That paper concluded that for the SMI method convergence rate is dependent only on the number of weights and is independent of the noise and interference environment. Many different algorithms came into existence after the SMI, but the SMI remained most widely used algorithm due to its simplicity. Kelly [9] improved on the SMI method of [8] by replacing the ad hoc procedure of Brennan and Reed by a likelihood ratio test. Other algorithms include eigenanalysis-based processing such as the principle component inversion (PCI) method [10] and the eigencanceler [11]. The sidelobe canceler (SLC) was suggested in [12]. The PCI method [10] is developed for low rank approximation of a data matrix. In [10], Kirsteins and Tuft provide a useful comparison between the PCI and the SMI methods. The paper proves that the PCI method has a higher convergence rate than the SMI. In this paper, the convergence rate is defined as the number of samples needed in adaptation process to achieve maximaum signal-to-noise ratio at the output. The authors state that a significant advantage of the PCI method is that it achieves more

rapid adaptation than conventional methods such as adaptive loops [6], [7], the SMI [8], and the generalized likelihood ratio test (GLRT) receiver of Kelly [9]. The eigencanceler in [11] utilizes the eigenstructure of space-time covariance matrix to adapt its weight vectors. The eigencanceler provides a good alternative to the SMI method due to its robustness and convergence speed. In [12], Hendon and Reed derives yet another algorithm called the constant false alarm rate (CFAR) sidelobe canceler (SLC). As the name suggests it has the CFAR feature embedded in it. An approach based on reducing the processor's number of degrees of freedom is suggested in [13]. In fact, the PCI method [10] and the eigencanceler [11] also reduce the number of degrees of freedom during weight adaptation. In [13], the weight computation is done in two steps. First, the interference covariance matrix is transformed into a lower rank matrix using a matrix created from singular vectors of covariance matrix and then, for newly created transformed matrix, weights are calculated. Chapman [14] and Van Veen and Roberts [15] describes several reduced rank adaptive beamformers. Chapman, in [14] reduces the number of adaptive channels by means of various configurations before calculating the weights. Contrary to [13], Chapman in [14] investigates each configuration further and provides evaluation of the effects of array errors on all configurations studied. The author also studied the effects of the finite transient response time on the effectiveness of the adaptive array for the case of a typical defense radar system. In [15], authors develops a partially adaptive beamformer design that minimizes output power.

The Type II of work according to our classification consists of extensions to original algorithms [16-22]. A multiband SMI (MBSMI) algorithm is proposed in [16]

as oppose to the single band SMI (SBSMI) of [8]. Here, authors state that the limitation of the SMI method is the size of secondary data record set, and point out that size of this data record could be increased by employing a frequency diversity scheme. They show that the MBSMI outperforms the SBSMI. They did so by comparing both methods under chosen system constraints. Articles [17-19] are extension works based on the Kelly's GLRT [9] receiver. In [17], [18], and [19] authors describe the multiband GLR, the joint domain localized GLR (JDL-GLR), and doppler domain localized GLR (DDL-GLR) receivers, respectively. All of the GLR extensions have desirable feature of the CFAR. The adaptive algorithm of [17] proves that it is better than the MBSMI even in the non-Gaussian environment such as Weibull, Log-normal, and K-distribution. In [18], superiority of the JDL-GLR is proven against space-time and time-space processor configurations in nonstationary and nonhomogeneous environments. In [19], authors Wang and Cai show that the DDL-GLR is a data-efficient implementation of higher order optimum detector.

Finally, the third type of papers, by our classification, provide comparisons among existing algorithms [20-25]. In [20], authors compared adaptive loops of Applebaum [6] to the SMI [8] and to another algorithm which is based on recursively updating the inverse of the sample covariance matrix. Authors of [20] show that the SMI provides better performance in terms of number of samples needed for weight computation than the other two methods. Chang and Yeh [21] compared the performance of the eigenspace-based beamformers to the SMI method. They showed that performance of the SMI method is degraded by the disturbed noise subspace due to the estimation process of the

covariance matrix and proved that in such case eigenspace-based beamformers adapt faster than the SMI. Chang and Yeh [21] provided theoretical as well as analytical results to prove superiority of the eigenspace-based beamformers. In [22], Cai and Wang described another extension of the SMI method called the modified SMI and provided its comparison to the GLR algorithms. The paper remarked that in Gaussian interference environment, the GLR receiver has a probability of false alarm independent of the unknown interference statistics, i.e. it has the CFAR feature; and in non-Gaussian environments such as the Weibull clutter, the GLR is much more robust than the Modified SMI. Papers [23] and [24] are related to each other in a sense that they both analyze Mean Square Error (MSE) performance of linearly constrained minimum variance beamformers. In [23], Van Veen analyze the case where same set of data is used for both, weight adaptation as well as output statistic formulation. Krolik and Swingler [24], on the other hand analyzes further to include the case when calculated weights from one set of data is applied to other distinct set of data. Both papers provide excellent mathematical analysis. Van Veen in [25] compares three partially adaptive beamformers, namely beam-based, eigenstructure-based, and power minimization based designs. He proves that the power minimization based design performs better than other two when the number of adaptive degrees of freedom is limited.

Our work falls into the third category approach. It provides the comparison among the SMI method [8], the eigencanceler [10], and the two step nulling technique [13]. The comparison is based on the convergence rate of the algorithm in terms of the normalized output signal-to-noise ratio, and detection capability of the algorithm. In this paper, the

two step nulling algorithm is referred to as the transformed SMI. The given name becomes self evident in chapter 4. The eigenvectors of the covariance matrix shall be used to transform the covariance matrix to a lower rank matrix. The present work will show that the transformed SMI and the eigencanceler have higher convergence rate than the SMI method. It will also show that the transformed SMI provides higher probability of detection than two of its competitors considered in this paper. The comparison will be done under linearly constrained environment.

The present work is organized as follows: Chapter 2 details the signal model used throughout the paper and also develops space-time covariance matrix. Chapter 3 discusses the classical Wiener filter and introduces various algorithms to be compared. Chapter 4 describes simulation model explains the simulation results obtained and chapter 5 draws conclusions. Appendix A provides analytical results for weight vector calculation of Eigencanceler and appendix B consists of simulation graphs.

CHAPTER 2

MATHEMATICAL MODEL

The general mathematical signal model will be derived which in turn will be utilized to formulate the space-time covariance matrix. The following notation has been adopted throughout the paper unless otherwise stated : boldface lower case letters denote vectors, boldface uppercase letters denote matrices, the superscript H denotes conjugate transpose - Hermitian transpose.

2.1   Signal Model

Consider an airborne array consisting of N omni-directional transmit/receive modules. Each module has a K-tap FIR filter associated with it as shown in the Figure 1.

The signal received from a point-like target is given by [11] :

$$s_r(t) = g(t - \tau_n) a(t) e^{j(\omega_c - \upsilon)(t - \tau_n)} \tag{1}$$

where g(t) is the transmitted waveform, a(t) represents the phase and amplitude of the received signal, τ_n is the propagation delay between the first and the n-th sensor, ω_c is the carrier angular frequency, and ϑ is the doppler angular velocity. For a linear uniform array the propagation delay is given by $\tau_n = l \sin \theta / c$, where l is the inter-element spacing, θ is bearing of the source measured from the normal of the array, and c is the speed of light. The doppler shift ϑ is given by $\vartheta = 2\upsilon_r \omega_c / c$, where υ_r is the radial velocity of the target. It is obvious that for a given target, the received signal $s_r(t)$

7
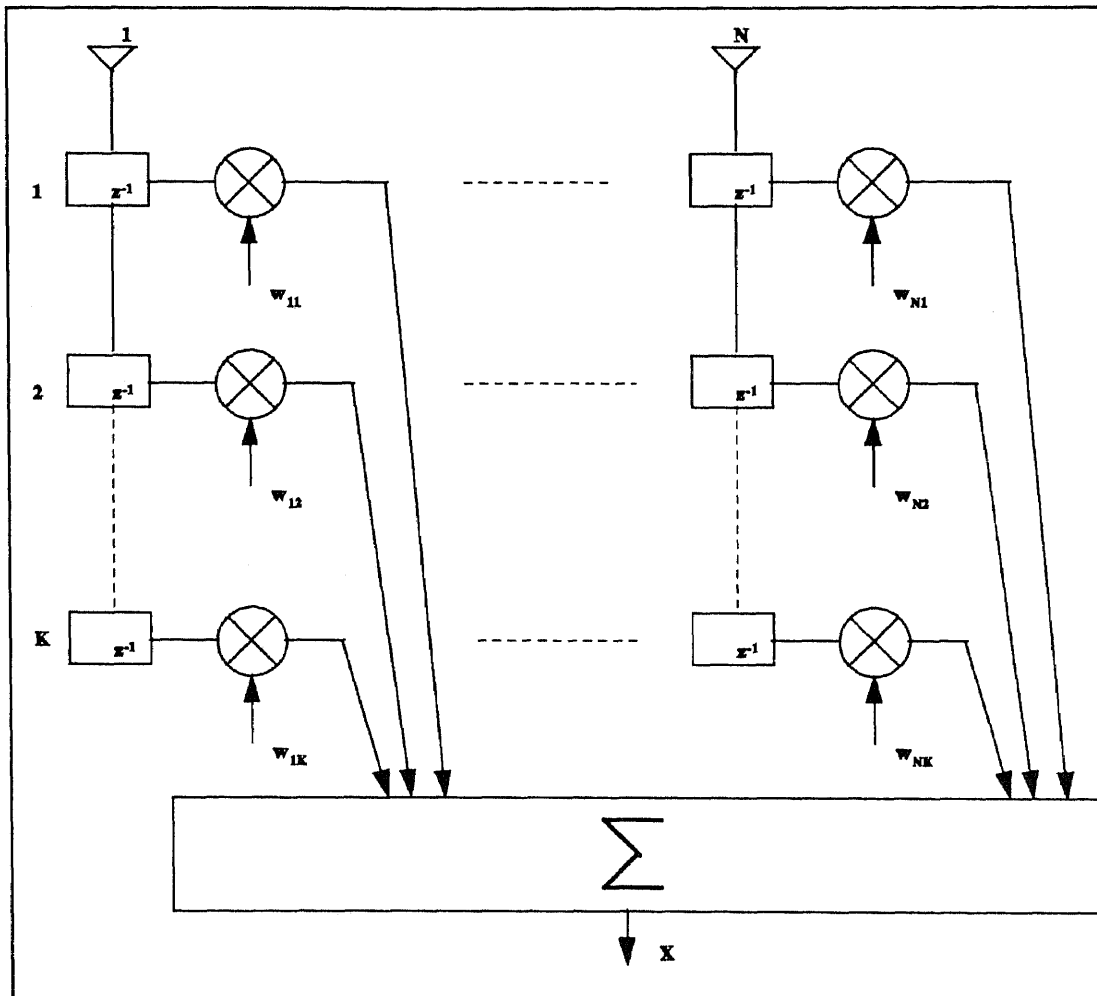
Figure 1: Generic Block Diagram of Adaptive Radar Receiver

depends on both, the angle θ and doppler frequency ϑ.

After achieving demodulation of the carrier signal, baseband signal shall have the following form.

$$s_n(t) = s_r(t)e^{-j\omega_c t}$$

$$= g(t - \tau_n)a(t)e^{-j(\omega_c \tau_n + \upsilon t - \upsilon \tau_n)} \tag{2}$$

The above expression can be further simplified by noting that $\vartheta << \omega_c$ and hence ignoring the term $\vartheta\tau_n << \omega_c\tau_n$. Also, a reasonable assumption could be made regarding g(t). It can be assumed that g(t) will be constant during the propagation time across the array, i.e. g(t - τ_n) = 1. Hence, we have,

$$s_n(t) = a(t)e^{-j(\omega_c \tau_n + \upsilon t)} \tag{3}$$

The term $u = \omega_c\tau_n$ represents the phase lag across the array due to the propagation delay. If the time interval between successive pulses is given by T_r, then $v = \vartheta T_r$, is the doppler phase shift between two successive pulses.

Now, we define a stacked position vector **d** as follows :

$$d(u,v) = \frac{1}{\sqrt{NK}}\left[1 \quad e^{-ju} \quad \cdots \quad e^{-j(N-1)u} \quad e^{-j((N-1)u+v)} \quad \cdots \quad e^{-j((N-1)u+(K-1)v)}\right] \tag{4}$$

where the scaling factor has been introduced to normalize the magnitude of the vector to unity. **d** is a function of both angle of arrival θ and the doppler frequency ϑ. Next, we write $s_n(t)$ as a vector in terms of stacked position vector **d**, and call it s(t)

$$s(t) = a(t)d(\theta,\upsilon) \qquad (5)$$

Equation (5) is a representation of a point source by a rank 1 vector. In cases when signals extend over a range of angles θ or doppler frequencies υ, we can choose discrete points in the range of interest and represent the signal as a superposition of rank 1 vectors.

2.2   Covariance Matrix

In general, the signal received at the array may consist of the target echo of interest s(t) and interferences such as jammer signals j(t), the clutter c(t), and the thermal noise n(t). Let N-dimensional array vector z(t) represent the sum of all contributions at the array output at time t, i.e. z(t) = s(t) + j(t) + c(t) + n(t) . The snapshot vector z(k) is the k-th sample of z(t). Let's define the stacked snapshot vector $X(k) = [z^T(k), z^T(k+1),..., z^T(k+K-1)]^T$. The temporal cross-correlation between two snapshots is given by:

$$r(p) = E\big[z(k)z(k-p)\big] \qquad (6)$$

The space-time covariance matrix is generated from the cross correlations at all available time lags.

$$R = E\Big[XX^H\Big]$$

$$R = \begin{bmatrix} r(0) & r(1) & \cdots & r(K-1) \\ r(-1) & r(0) & \cdots & r(K-2) \\ \vdots & \vdots & \ddots & \vdots \\ r(-K+1) & \cdots & r(-1) & r(0) \end{bmatrix} \qquad (7)$$

CHAPTER 3

VARIOUS ALGORITHMS

The theory of adaptive radar was established in a series of publications by Brennan, Mallett, and Reed [7],[20]. They showed that if the disturbance is a stationary process and the elements of the corresponding array vector are distributed jointly Gaussian, then the likelihood ratio test for detecting the signal in the presence of the interference is maximized by processing the data with the following weight vector,

$$w_o = kR^{-1}d_s \tag{8}$$

where d_s is the position vector corresponding to the desired signal and k is a gain constant. Equation (8) represents the classical Wiener Filter. The corresponding weight vector is optimum if the covariance matrix R is known. In practical situation a-priori knowledge of the space-time covariance matrix is unavailable since we have to work with finite window of data from which R must be estimated. In this case the solution is not optimum. And the quality of solution depends upon the fact that how close the estimated covariance matrix is to the real covariance matrix.

The signal environment can be assumed stationary only over short periods. Hence, the covariance matrix estimate needs to be continually updated. Because of changing environment, the same weight vector can not be used for different data sets if better detection capability is the goal. Many adaptive algorithms have been developed over the

12

years for updating the array weight vector. The following are the three algorithms that are compared in this paper.

3.1   Sample Matrix Inversion (SMI)

Originally proposed by Reed, Mallett, and Brennan [8], SMI is quite popular for its simplicity. As pointed out earlier, the knowledge of space-time covariance matrix is not available in practice. So, an estimate of the covariance matrix is achieved and used.

The covariance matrix can be estimated using the relation :

$$M = \frac{1}{I}\sum_{i=1}^{I} x_i x_i^H \tag{9}$$

where I is data record size and x_i are the various snapshots corresponding to different sample times. This estimated matrix **M** is used in equation (8) to calculate the weight vectors and thus, the name Sample Matrix Inversion algorithm.

$$w_{SMI} = kM^{-1}d_s \tag{10}$$

The constant k in above equation depends on the constraint placed to achieve prescribed response over a range of angles and doppler frequencies. The weight vector is then obtained by solving the linearly constrained minimization problem.

$$\min_{w} \quad w^H M w \text{ subject to constraint } C^H w = f \tag{11}$$

where **C** is the NK X J constraint matrix and f is the desired response vector. Gradient of equation (11) provides,

$$J = w^H M w + \mu(w^H C - f^H)$$

$$Now, \quad \nabla = \frac{\partial J}{\partial w^H} = Mw + \mu C = 0$$

$$w = -M^{-1}C\mu \tag{12}$$

substitute w into $C^H w = f$,

$$-\mu C^H M^{-1}C = f$$

$$\mu = -\frac{f}{C^H M^{-1}C}$$

substituting μ into equation (12), we get

$$\therefore \quad w_{smi} = M^{-1}C(C^H M^{-1}C)^{-1}f \tag{13}$$

For the purpose of this paper, the constraint of the unity gain in the direction of look has been adapted. Thus,

$$C = \mathbf{d_s} \; ;$$

$$f = 1 \; ;$$

which in turn implies,

$$w_{smi} = \frac{M^{-1}d_s}{d_s^H M^{-1}d_s} \tag{14}$$

In theory, as I in equality (9) approaches infinity, the estimated covariance matrix **M** approaches **R**. No doubt that the SMI is simplest algorithm of all but its simplicity is

achieved by trading the convergence speed. Here, in the entire paper, the convergence speed is defined as the number of samples needed during weight adaptation to achieve maximum signal-to-noise ratio at the output. As eq.(14) shows, calculation of weight vector requires a matrix inversion which requires an order of $(NK)^3$ multiplications. Obviously $(NK)^3$ could be quite large even for moderate number of filters and filter taps. The eigencanceler is an algorithm that does not require direct matrix inversion. The algorithm utilizes eigenstructure of the space-time covariance matrix to determine the weight vectors as described below.

3.2   Eigencanceler

Before proceeding with the calculation of the weight vectors, it is important to explore some important properties of the space-time covariance matrix since they hold the essence of this particular method.

3.2.1   Eigenstructure of the Space-time Covariance Matrix

In radar applications, the desired signal (pulse reflected from target) is present only part of the time. Considerable simplification can be achieved if the interferences are estimated when the desired signal is not present. This corresponds to collecting clutter and jammer data from neighboring range cells. For this case, the stacked array vector x(t) is a superposition of clutter signals c(t), jammer signals j(t), and the thermal noise n(t). The space-time covariance matrix can be written also as a superposition of the clutter, the jammer, and the noise covariance matrices.

$$M = E\left[XX^H\right]$$

$$= M_C + M_J + M_N \tag{15}$$

It would be reasonable if we assume that there exists no correlation between the clutter echoes, jammer signals, and thermal noise. To investigate the eigenstructure, we will have to examine each contributor in more detail [1].

Clutter : The clutter extends over a sector of angles Θ and due to the flight geometry of the airborne radar, it covers a band of doppler frequencies. The clutter covariance matrix is given by

$$M_C = \int_\Theta \int_{B_v} p_c(\theta,\upsilon)\bar{d}(\theta,\upsilon)\bar{d}^H(\theta,\upsilon) \; d\upsilon \, d\theta \tag{16}$$

where $p_c(\theta,\upsilon)$ is the power spectral density of the clutter at angle θ and doppler frequency υ.

Jammers : Jammer signals can be viewed as sources at discrete angles. In general, we can model jammers to extend over the full range of baseband frequency, since this range B_υ, is much smaller than RF frequency at which the jammer signals are originated. The jammer covariance matrix can be written as

$$M_J = \sum_{\theta_i} \int_{B_v} p_{J,i}(\upsilon) \; \bar{d}(\theta_i,\upsilon)\bar{d}(\theta_i,\upsilon) \; d\upsilon \tag{17}$$

where $p_{J,i}(\upsilon)$ is the power spectral density of the ith jammer and at the frequency υ.

Noise :   Thermal noise is assumed white across the array and over

the frequency band of interest.   In other words, sensor outputs are

uncorrelated to each other and uncorrelated to themselves at non-zero time

lag. The resulting covariance matrix is the unity matrix scaled by the noise

variance :

$$M_N = \sigma_N I \tag{18}$$

From above discussion it is evident that, in the airborne radar problem, clutter and

jammer signals may be broadband spatially as well as temporally. The eigenstructure of

the space-time covariance matrix for such signals has been considered by number of

authors, [26], [27]. They concluded that the space-time matrix is characterized by a

limited number of dominant eigenvalues and a large number of small eigenvalues.

Buckley [27] states an argument that relates the number of dominant eigenvalues to the

array time-bandwidth product. This product is calculated from the duration of the signal

across the array/filter taps structure and bandwidth of the signal and is equal to (N + K -

1). Examples of typical eigenspectra resulting from a clutter field and background noise

are shown in Figure 2 for different data record sizes : NK, 1.5NK, 2NK, 3NK, 5NK, and

10NK. The curves were obtained using the simulation model described in chapter 5.

The total power of all the signals in the array is given by :

$$P = tr[M] = \sum_{i=1}^{NK} \lambda_i \tag{19}$$

where λ_i are the eigenvalues of space-time covariance matrix M indexed in ascending

order (λ_1 is the largest eigenvalue). By inspection of Figure 2, we can conclude that most

of the power is compacted in the largest (N + K - 1) eigenvalues. For arrays in which

(N + K - 1) << NK, a small number of eigenvalues contain all the information about

interferences. It follows that the span of the eigenvectors associated with the dominant

eigenvalues include all the position vectors that comprise data. For that reason, we refer

to the dominant eigenvectors as interference eigenvectors. The space spanned by

interference eigenvectors is called the interference subspace. The non-dominant

eigenvectors, called noise eigenvectors which span the noise subspace, are orthogonal to

dominant eigenvectors, and hence, are orthogonal to interference subspace.

3.2.2   Weight Vector Calculation

Let Q_r denote the matrix representation of the interference subspace, generated by the

jammers and clutter contributions. The columns of Q_r consist of the interference

eigenvectors. Let Q_v denote the matrix representation of the noise subspace. The

columns of Q_v consist of the noise eigenvectors. Since $Q_r^H Q_v = 0$, any weight vector in

the noise subspace, $w \in$ span$\{Q_v\}$, has the property of nulling-canceling interferences.

The interference cancellation process consumes only a limited number of degrees of

freedom, namely (N + K - 1). Additional requirements may be imposed on w to optimize

some array performance criterion. Two beamformer formulation are suggested [11] : The

minimum power eigencanceler (MPE) and the minimum norm eigencanceler (MNE). In

this paper only the MNE is investigated.

The minimum norm eigencanceler (MNE) is designed to minimize the norm of the

weight vector while maintaining the linear and eigenvector constraints :

$$\min_{w} \quad w^H w \; \text{subject to} \; Q_r^H w = 0 \; \text{and} \; C^H w = f \tag{20}$$

The solution to the optimization problem in equation (20) is provided in Appendix A. In appendix A, we show that :

$$w_e = Q_v Q_v^H C \left[C^H Q_v Q_v^H C \right]^{-1} f \tag{21}$$

Since, $Q_r Q_r^H + Q_v Q_v^H = I$, we get

$$w_e = (I - Q_r Q_r^H) C \left[C^H (I - Q_r Q_r^H) C \right]^{-1} f \tag{22}$$

which represents weight vector in terms of dominant eigenvectors.

Now substituting $C = d_s$ and $f = 1$, we get

$$w_e = (I - Q_r Q_r^H) d_s \left[d_s^H (I - Q_r Q_r^H) d_s \right]^{-1} \tag{23}$$

3.3 Transformed SMI

As the name of the method suggests, it is another form of Sample Matrix Inversion method but with added strength of the principle component inversion (PCI) method. The author of this method, Marshall [14], called it the two step nulling. The description of this method and derivation of weight vector are as follows :

First, the estimated space-time covariance matrix is generated from the set of observation vectors using relation (9). Then, eigenfactorization is achieved in a similar fashion as in the eigencanceler. The interference subspace Q_r consisting of dominant eigenvectors is achieved.

Let's define a transformation matrix T as

$$T = \begin{bmatrix} q_1, & q_2, & \cdots & , q_p, & d_s \end{bmatrix} \qquad \textit{where } p = 1,2,...,2(N+K) \qquad (24)$$

where d_s is the steering vector and q_i's are dominant eigenvectors of estimated covariance matrix **M**. The transformation matrix **T** has the dimension of NK X (p+1). This transformation matrix is then used to transform the space-time covariance matrix M as follows :

$$D = T^H M T \qquad (25)$$

Where **D** is the transformed space-time covariance matrix. **D** has some interesting characteristics that should be mentioned.

1. **D** is a reduce-ranked matrix with rank equal to (p+1) . On the other hand **M** had a rank of NK > (p+1).

2. **D** belongs to interference subspace only.

The first characteristic contributes to the speed of the algorithm as it is less computational burden to invert (p+1) X (p+1) matrix than to invert NK X NK matrix. The second characteristic guarantees the interference cancellation capability.

Similarly, the desired position vector is also transformed with **T**. The new position vector, call it d_t is,

$$d_t = T^H d_s \qquad (26)$$

Now, using these transformed parameters, the weight vector for this algorithm is formed.

$$\min_{w} \ w^H D w \ \textit{subject to} \ d_t^H w = 1 \qquad (27)$$

The solution to the problem in (26) is,

$$w_t = \frac{D^{-1}d_t}{d_t^H D^{-1}d_t} \qquad (28)$$

The above weight vector has a dimension of (p+1) X 1.

CHAPTER 4

NUMERICAL RESULTS

For the ease of programming we considered a linear uniform array with N = 8 elements. The separation between two array element was kept at half wavelength. Each channel consisted of an FIR filter with K = 4 taps. The sampling frequency was normalized to unity. The radar waveform was modeled such that it could be considered constant over the propagation time across the array. An airborne radar, with a platform velocity of 0.4 was modeled. Hence, the ground clutter at boresight appears approaching at relative velocity of 0.4. The clutter was assumed to extend over the full angular sector considered (-90° to +90°). The clutter returns were simulated by spreading 30 scatterers at random in the considered angular sector. The clutter echoes were modeled as independent complex Gaussian random variables, with zero mean and variance determined by the clutter-to-noise Ratio (CNR). The CNR was calculated from the contributions of all clutter echoes. The clutter generated using above guidelines might have distribution shown in the Figure 3. The simulation also included two jammers located at -30° and 10°, with jammer-to-noise Ratios (JNR) of 20 dB and 10 dB, respectively. Both jammers were modeled approaching at relative redial velocity of 0.8. The noise was modeled as white with variance of unity.

Using the definition of stacked position vector, the observation vector **X** was calculated which consisted of clutter echoes, jammer signals, and thermal noise under

interference only hypothesis and it included signal term also under signal plus interference hypothesis. Number of observation vectors were collected for different data record sizes. Here data record sizes of NK, 1.5NK, 2NK, 3NK, 5NK, and 10NK are being considered. Following calculation was done for every set.

First, space-time covariance matrix was derived from eq. (7). Using the observation vectors under interference only hypothesis the estimated covariance matrix was calculated from eq. (9). Then, various weight vectors were calculated for herein considered methods. For Eigencanceler and Transformed SMI method, the assumed rank p of interference subspace matrix Q_r was varied from 1 to 2(N + K). For all of these different sizes of p, weight vectors were calculated for both methods.

These weight vectors were used to calculate output of filter $y = w^H X$, where X belongs to signal plus interference hypothesis set. The calculation for mean and variance of y conditioned on w followed which in turn were used to formulate the normalized signal-to-interference ratio, ρ at the output of the filter. The normalized signal-to-interference ratio is defined as,

$$\rho = \frac{SIR \ for \ given \ method}{optimal \ SIR} \tag{29}$$

where SIR is the signal-to-total interference ratio.

The probability density function of ρ and probability of detection were also calculated and graphed. The probability density functions curves are obtained from the histograms and probability detection curves are obtained when the probability of false alarm is kept constant at 10^{-5}. The adopted antenna patterns for all methods were

achieved. The results of the simulation is discussed in the following section. All the results were obtained from averaging 200 independent runs of simulation.

Numerical results are disseminated in Figures 2 through 23 in Appendix B. The grouping of these results is done as follows: Figures 2 and 3 show the eigenvalue plots and clutter spectrum, respectively. Figures 4 through 9 display graphs of normalized signal-to-noise ratio, ρ at the filter output with respect to the assumed rank of interference subspace. In this set of plots, each figure represents outcome of simulation for various data record sizes. Different data record sizes used are NK, 1.5NK, 2NK, 3NK, 5NK and 10NK. Figures 10 through 15 show probability density function of ρ, and Figures 16 through 21 are probability of detection curves. For these two sets also variable between two curves is data record size. Figures 22 and 23 are frequency and angle pattern curves, respectively.

Brief description of these numerical results is given in following paragraphs.

Normalized signal-to-noise ratio curves: (Figures 4 through 9)

Examination of these figures reveal that the transformed SMI and the eigencanceler provide higher normalized signal-to-noise ratio than SMI, especially for small data record sizes (Figures 4, 5). Reed [8] proved in his paper that the SMI requires approximately 2NK snapshots to achieve half the performance of optimum processor. Indeed, from Figure 6, it can be seen that the SMI achieves normalized signal-to-noise ratio of approximately 0.53 at the data record size of 2NK. Examination of these plots, (Figure 7, for example) reveal that the transformed SMI and the eigencanceler obtain maximum achievable value of ρ when the value of the assumed rank of the interference subspace

is in close proximity of 7. This criteria is explained from Figure 2. It can be observed from Figure 2 that the number of dominant eigenvalues is approximately seven. This value is the true rank of the interference subspace. Indeed, the performance of the eigenanalysis-based methods peaks when the assumed rank p equals the true rank. The remaining curves (Figures 8, 9) imply that as the data record size increases, the performance of the SMI method improves. These figures also show that the SMI has slow rate of convergence than the transformed SMI and the eigencanceler. Here, convergence rate is measured in terms of number of snapshots need for weight calculation. From Figure 9, we can see that the SMI requires 10NK snapshots to achieve ρ comparable to the transformed SMI and the eigencanceler.

Probability density curves: (Figures 10 through 15)

The examination of this set of plots also prove that the transformed SMI and the eigencanceler provide better performance in terms of ρ than the SMI method. It can be seen from the Figure 10 that the mean values of ρ for the transformed SMI and the eigencanceler are approximately 0.65 and 0.60, respectively, whereas the mean value of ρ for the SMI is approximately 0.05. As the number of snapshots increases, the mean value of ρ for the SMI improves. Figures 11 and 12 show that the mean value of ρ for the SMI is approximately 0.35 and 0.5, respectively. And, as the value of data record size gets very large, the mean value of ρ for all three method discussed here gets in close proximity (Figure 15).

Probability of detection curves: (Figures 16 through 21)

This set of curves again prove the superiority of the transformed SMI and the eigencanceler over the SMI method. The SMI method follows the same pattern as it did in previous results. That is, as the number of snapshots increases, the SMI provides better performance which is higher probability of detection for this set of plots.

Figure 22 represents frequency pattern curves for these methods. It can be observed from the figure that the transformed SMI nulls the clutter better than the eigencanceler and the SMI. The clutter, as we programmed is located at normalized frequency of 0.4 .

Finally, Figure 23 shows angle pattern curves for methods considered in this paper. We can clearly see the nulls placed at -30° and 10° where the jammer signals are suppose to be located.

To better understand the behavior of each method as revealed by the simulation results, we use the SMI method as a baseline for our discussion.

The weight vector for the SMI is given by equation (7) and rewritten below for convenience.

$$w_{sm} = kM^{-1}d_s$$

Now, M could be written as

$$M = Q_p\Lambda_pQ_p^{H} + Q_r\Lambda_rQ_r^{H} \tag{30}$$

where Q_p and Q_r represent interference and noise subspace matrix, respectively and Λ_p and Λ_r are interference and noise eigenvalue matrices, respectively. Then,

$$M^{-1} = Q_p \Lambda_p^{-1} Q_p^H + Q_r \Lambda_r^{-1} Q_r^H$$

where μ is a constant related to the type of constraint placed on the algorithm.

It follows that,

$$w_{SMI} = \mu \left[Q_p \Lambda_p^{-1} Q_p^H + Q_r \Lambda_r^{-1} Q_r^H \right] d_s$$

It is evident from the above representation of the weight vector equation that the weight vector for SMI consists of components from noise subspace as well as interference subspace. Graphical representation of the weight vector could be given as in Figure (24). Now, we noticed earlier that the SMI provides poor performance for small data record sizes (Figures 1, 2). For small data records sizes, the noise eigenvalues of the estimated covariance matrix are not constant. That is, they fluctuate substantially from one data set to the other (see curves for data record sizes NK and 1.5NK between the eigenvalue number 7 and 32 in Figure 2). This variation introduces the noise in the approximation process of the covariance matrix which, in turn leads to lower signal-to-noise ratio. As the number of snapshots grows the fluctuation in the noise eigenvalues decreases leading to the better approximation and the better performance (compare Figures 4 and 9).

In case of the eigencanceler, the equation for the weight vector is rewritten below. It is evident from the following equation that the weight vector only utilizes interference subspace for adaptation.

$$w_e = (I - Q_r Q_r^H) d_s \left[d_s^H (I - Q_r Q_r^H) d_s \right]^{-1}$$

Because of that the effect of the estimation noise is not realized in the eigencanceler and hence, it provides better signal-to-noise ratio than the SMI method for small data records.

The transformed SMI also utilizes the interference subspace, in this transformed interference subspace. And, thus provides better performance.

We observed from the normalized signal-to-noise ration curves, Figure 6, for example, that the performance of the transformed SMI matches the performance of the eigencanceler as long as the assumed rank of the interference subspace in less than or equal to the actual rank which is approximately seven. But when the assumed rank of the interference subspace is overestimated, the performance of the transformed SMI does not deteriorate as quickly as of the eigencanceler. This is due to the transformation that takes place in the Transformed SMI method before weight adaptation. The embodied steering vector d_s in the transformation matrix T ensures at the output that signal component in the observation vector does not get cancelled. More simply stated, the weight vector solution of the eigencanceler is not optimum in the subspace whereas the weight vector solution of the transformed SMI is optimum in the reduced rank subspace. Hence, the performance of the transformed SMI does not deteriorate as quickly as of the eigencanceler.

CHAPTER 5

CONCLUSION

In this paper, we examined three adaptive array techniques, namely the SMI, the eigencanceler, and the transformed SMI. We showed by simulation that the algorithms not requiring direct matrix inversion provide faster convergence rate. Here, convergence rate is defined in terms of normalized signal-to-noise ratio at the filter output. The paper proved that the transformed SMI and the eigencanceler provide superior performance than the SMI method for small data record sizes. The paper also showed that the transformed SMI provides better performance than the eigencanceler when the assumed rank of the interference subspace is overestimated. That is, the transformed SMI is robust to rank overestimation. The simulation also showed that the transformed SMI and the eigencanceler have relatively higher probability of detection for small data records. Again, we conclude that transformed SMI and the eigencanceler could be good alternatives to the SMI method, specially for short data record sizes.

APPENDIX A

EIGENCANCELER WEIGHT VECTOR CALCULATION

In this appendix we develop the expressions for weight vectors for the minimum norm eigencanceler (MNE).

The MNE weight vector is the solution to the optimization,

$$\min_{w} \quad w^H w \text{ subject to } Q_r^H w = 0 \text{ and } C^H w = f \tag{31}$$

Using the method for Lagrange multipliers, we define

$$J = w^H w - \left[w^H C - f^H \right] \lambda - w^H Q_r \mu \tag{32}$$

Taking gradient with respect to w^H,

$$\nabla = \frac{\partial J}{\partial w^H} = w - C\lambda - Q_r \mu = 0$$

which implies that,

$$w = C\lambda + Q_r \mu \tag{33}$$

Substituting above w into both of the above constrains, we get

$$Q_r^H C\lambda + Q_r^H Q_r \mu = 0$$

$$\mu = -Q_r^H C\lambda \tag{34}$$

where we have used a fact that $Q_r^H Q_r = I_r$, an identity matrix.

30

$$C^H C \lambda + C^H Q_r \mu = f \tag{35}$$

substituting μ, we get

$$C^H C \lambda - C^H Q_r Q_r^H C \lambda = f$$

$$\lambda \left(C^H C - C^H Q_r Q_r^H C \right) = f$$

$$\lambda = \left[C^H Q_v Q_v^H C \right]^{-1} f \tag{36}$$

where we have used the equality $Q_r Q_r^H + Q_v Q_v^H = I$

substituting λ and μ back we get,

$$w_e = Q_v Q_v^H C \left[C^H Q_v Q_v^H C \right]^{-1} f \tag{37}$$

APPENDIX B

SIMULATION RESULTS

This appendix consists of graphs generated by using the simulation model described in Chapter 5.
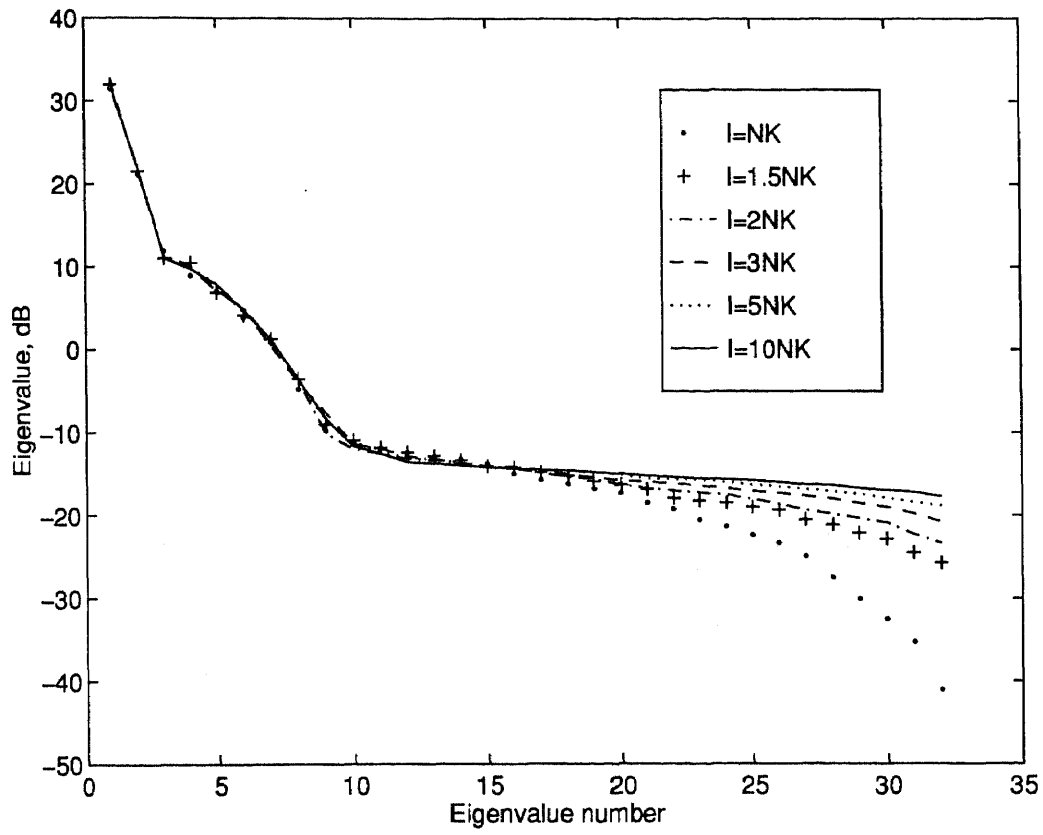
Figure 2: Eigenvalue Spectra
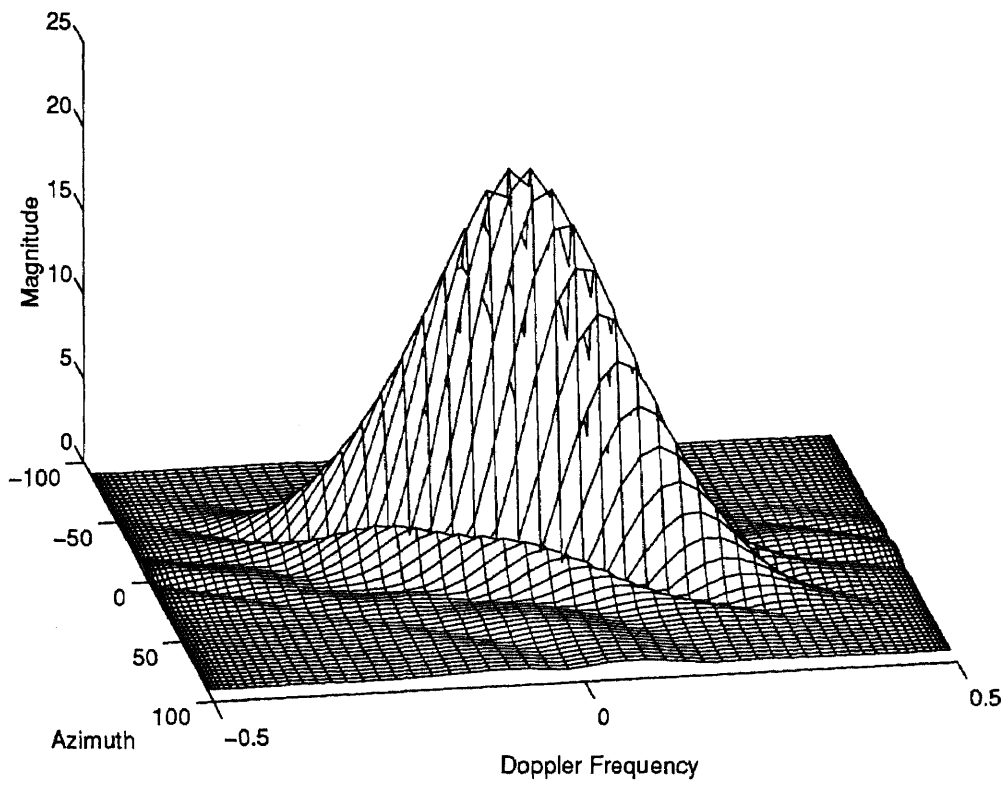
Figure 3: Clutter Spectrum
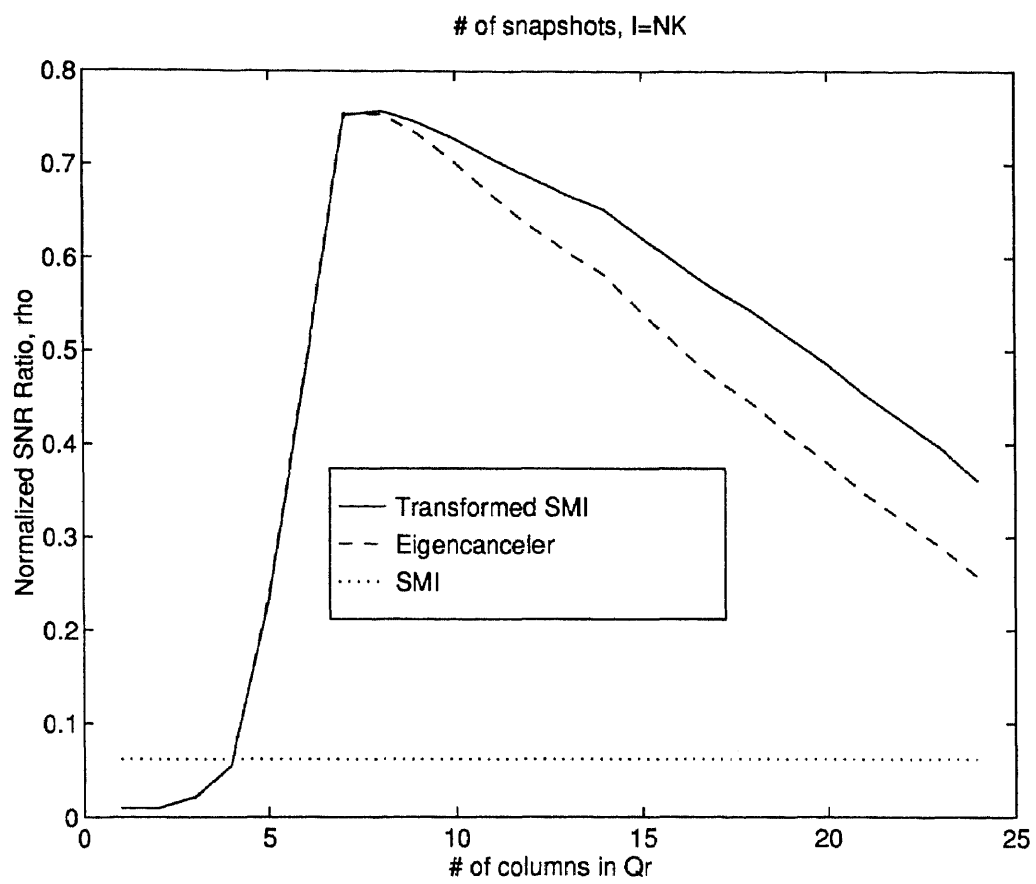
Figure 4: Normalized Signal-to-Noise Ratio, ρ (I = NK)
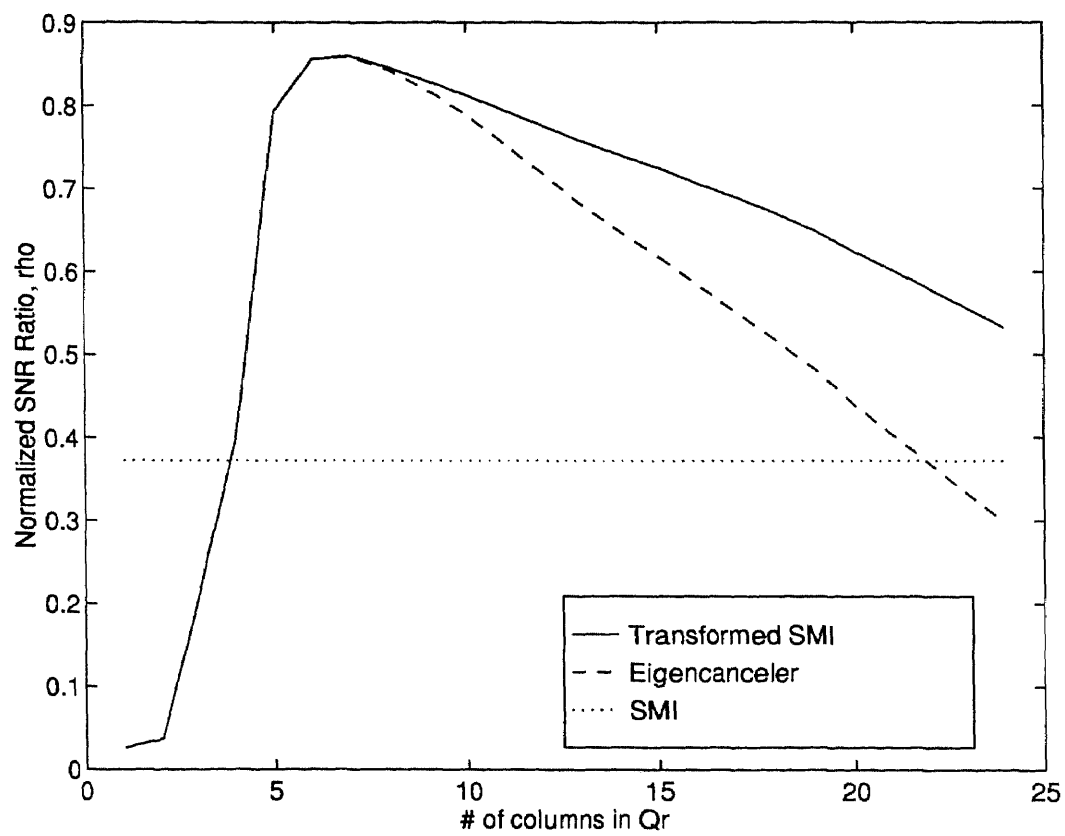
Figure 5: Normalized Signal-to-Noise Ratio, ρ (I = 1.5NK)
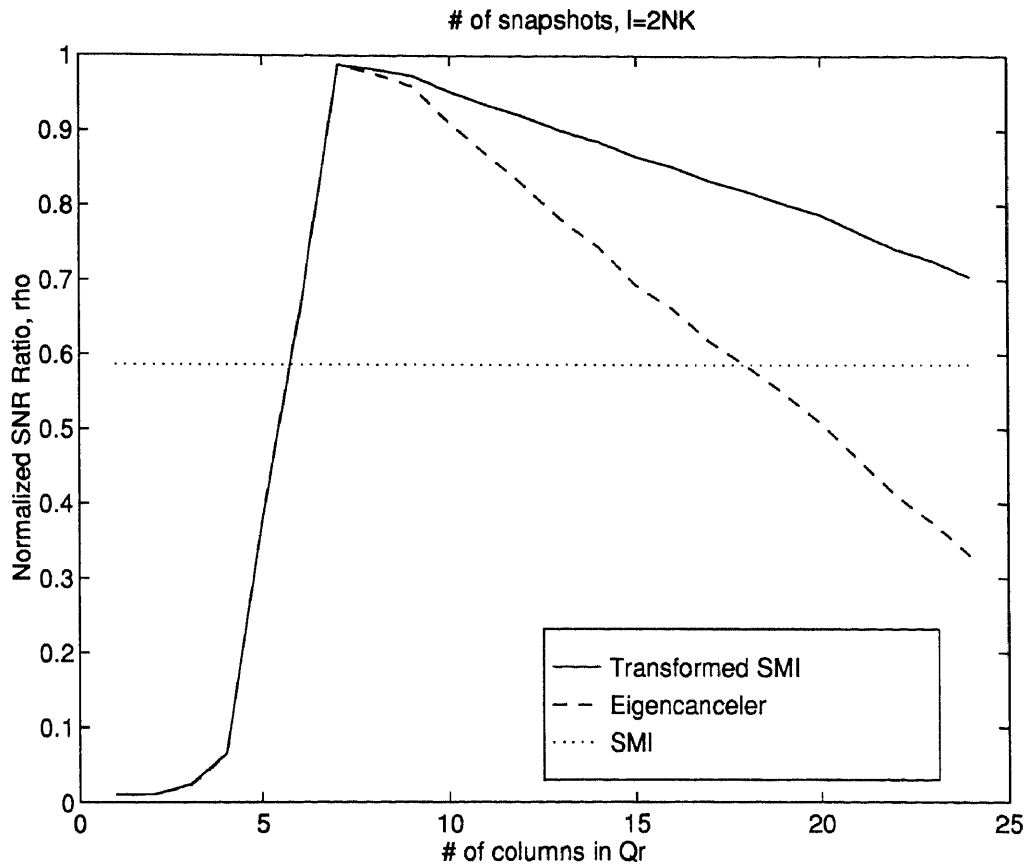
Figure 6: Normalized Signal-to-Noise Ratio, ρ (I = 2NK)
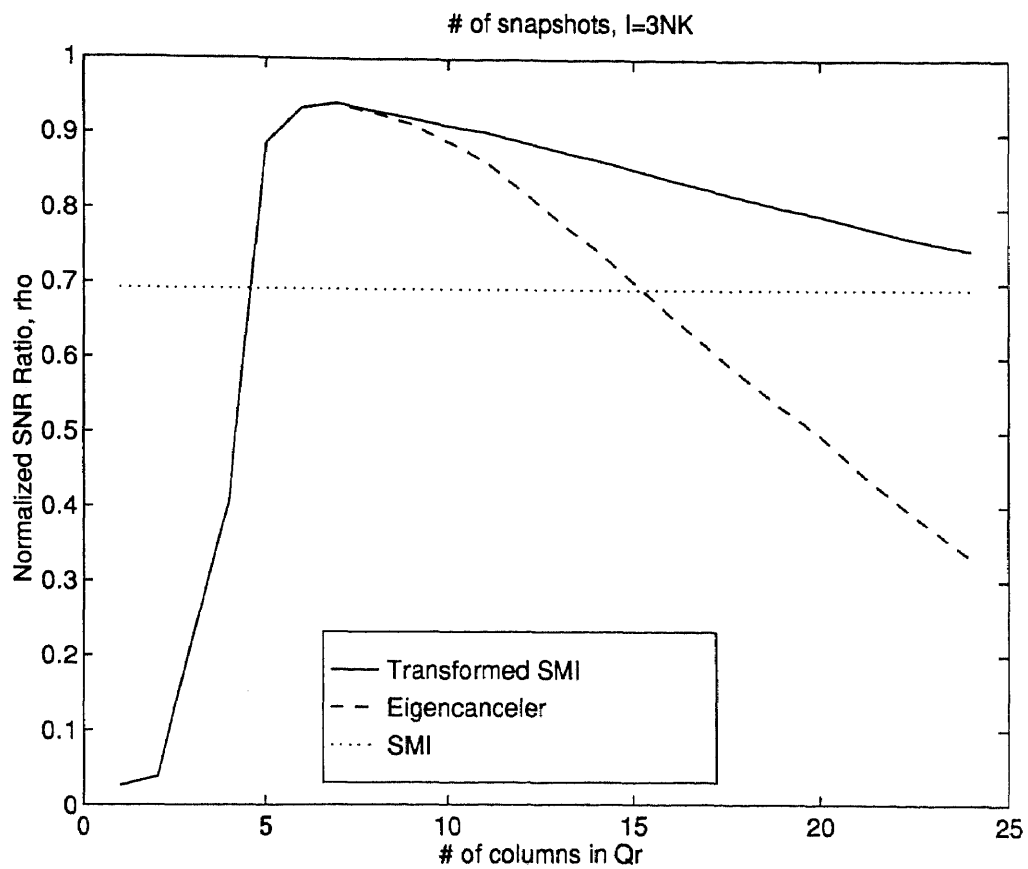
Figure 7: Normalized Signal-to-Noise Ratio, ρ (I = 3NK)
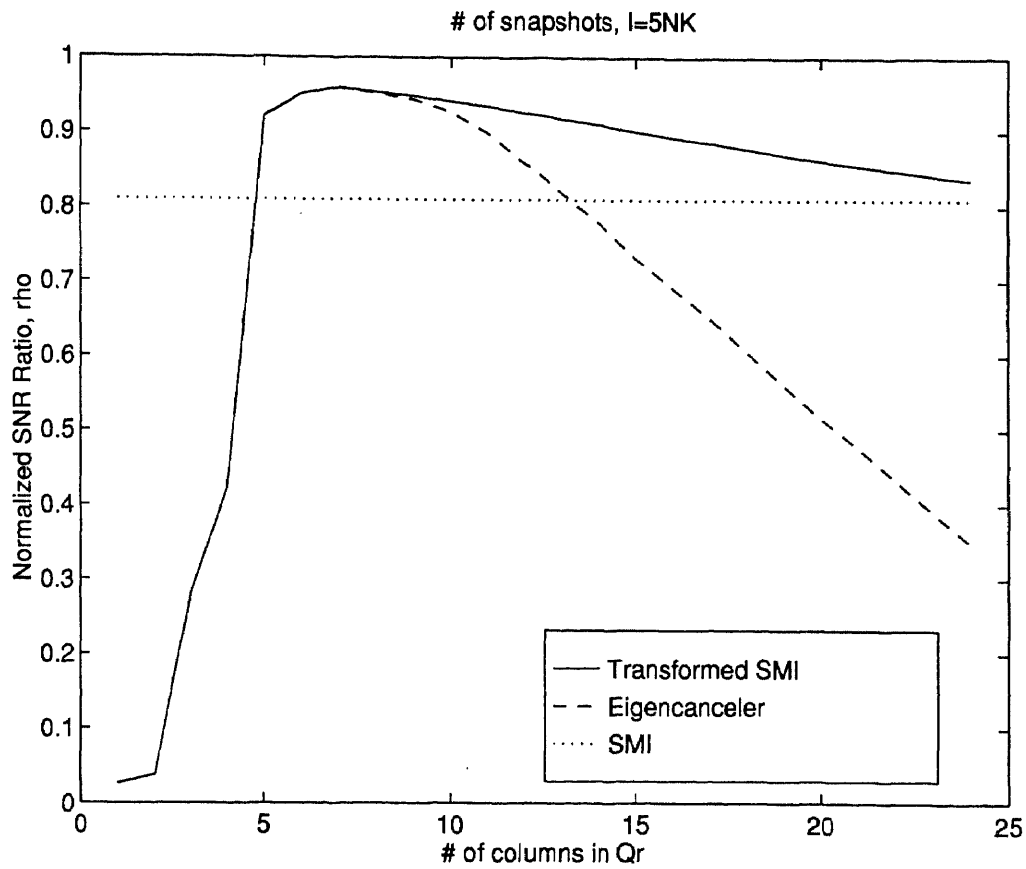
Figure 8: Normalized Signal-to-Noise Ratio, ρ (I = 5NK)
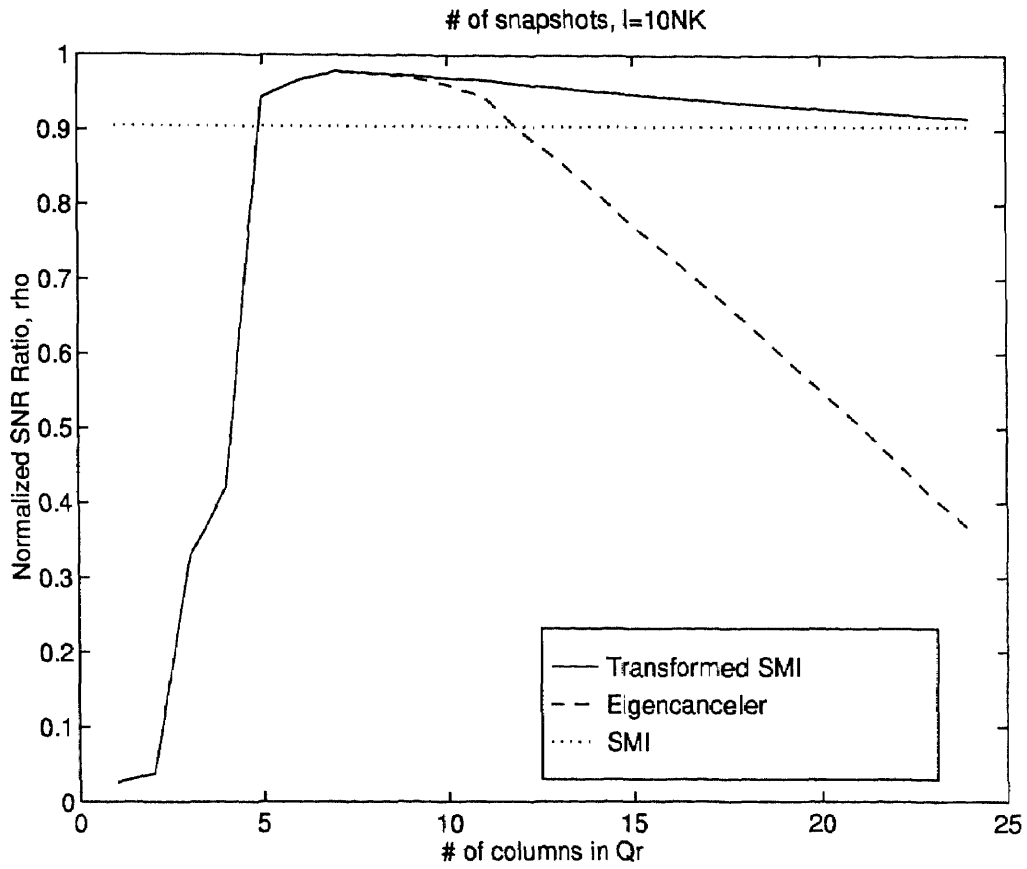
Figure 9: Normalized Signal-to-Noise Ratio, ρ (I = 10NK)
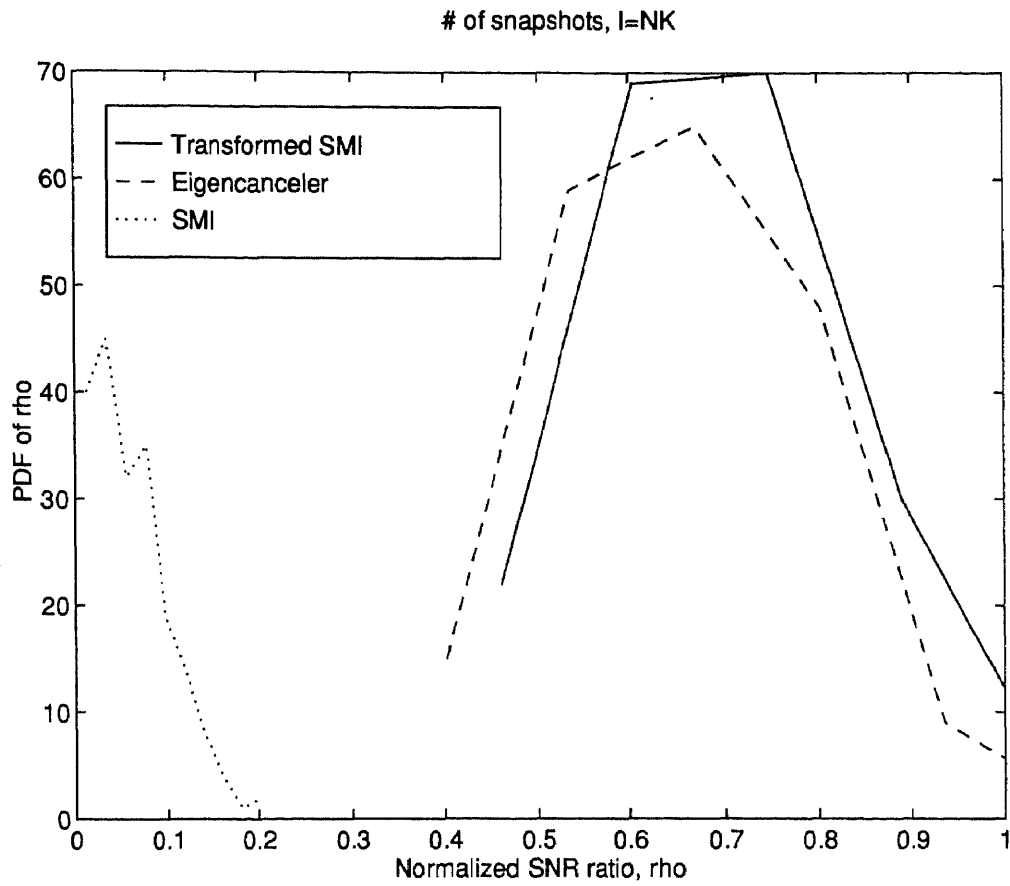
Figure 10: Probability Density Function of ρ, (I = NK)

# of snapshots, I=1.5NK
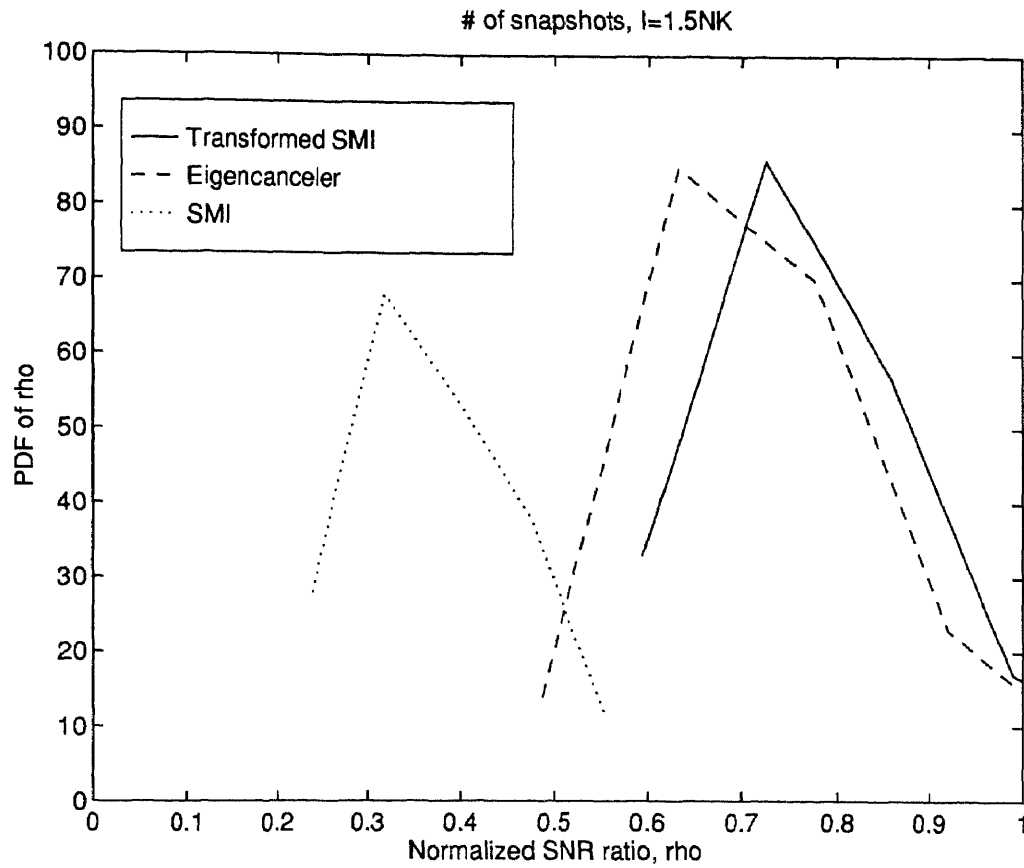
Figure 11: Probability Density Function of ρ, (I = 1.5NK)

# of snapshots, l=2NK
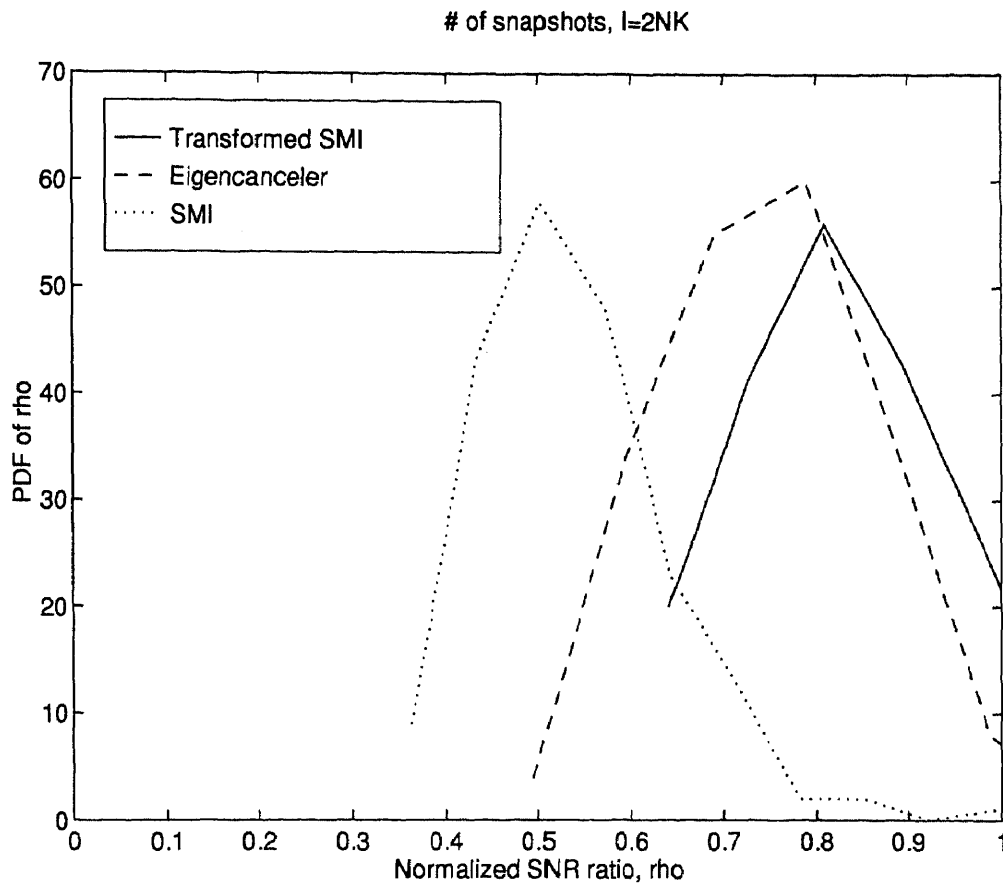
Figure 12: Probability Density Function of ρ, (I = 2NK)
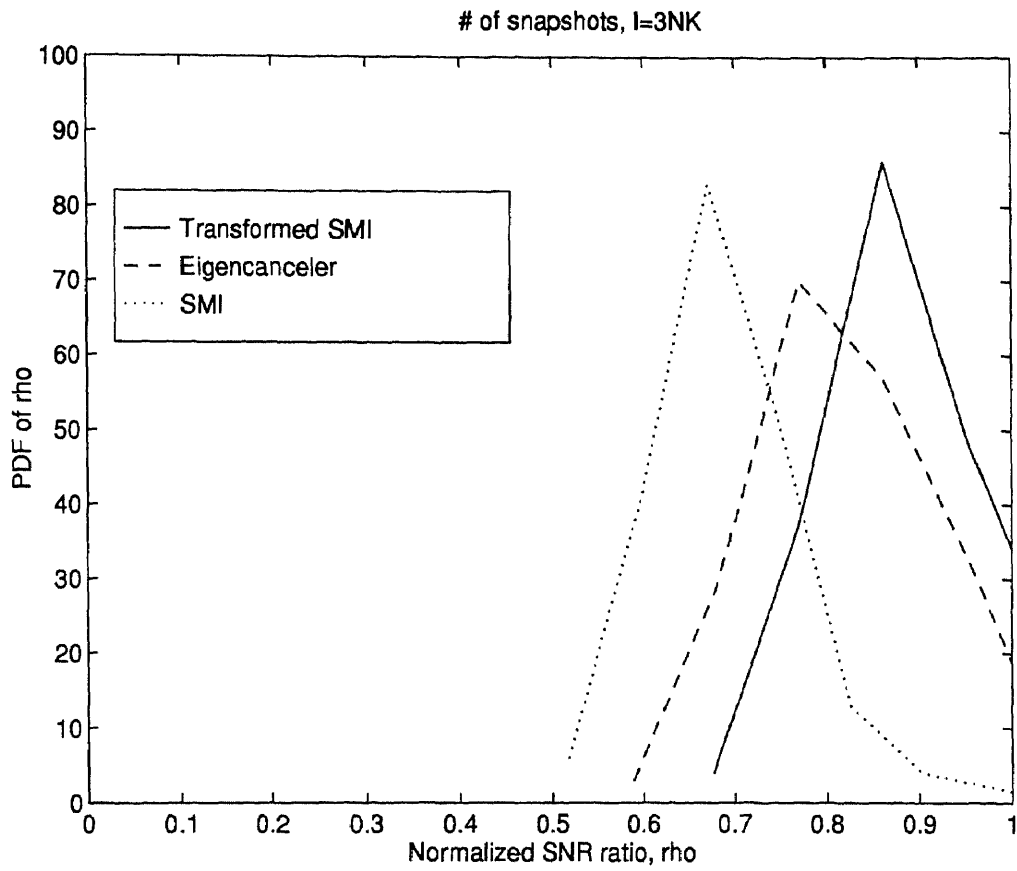
Figure 13: Probability Density Function of ρ, (I = 3NK)
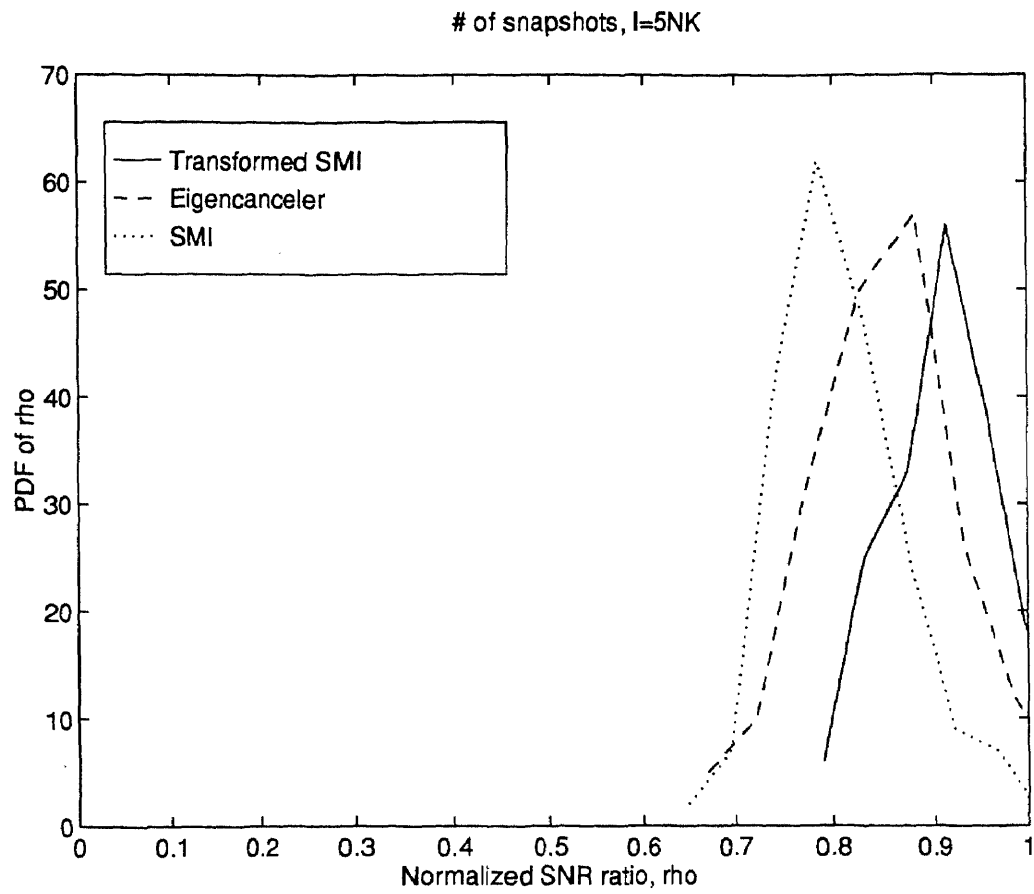
Figure 14: Probability Density Function of ρ, (I = 5NK)

# of snapshots, I=10NK
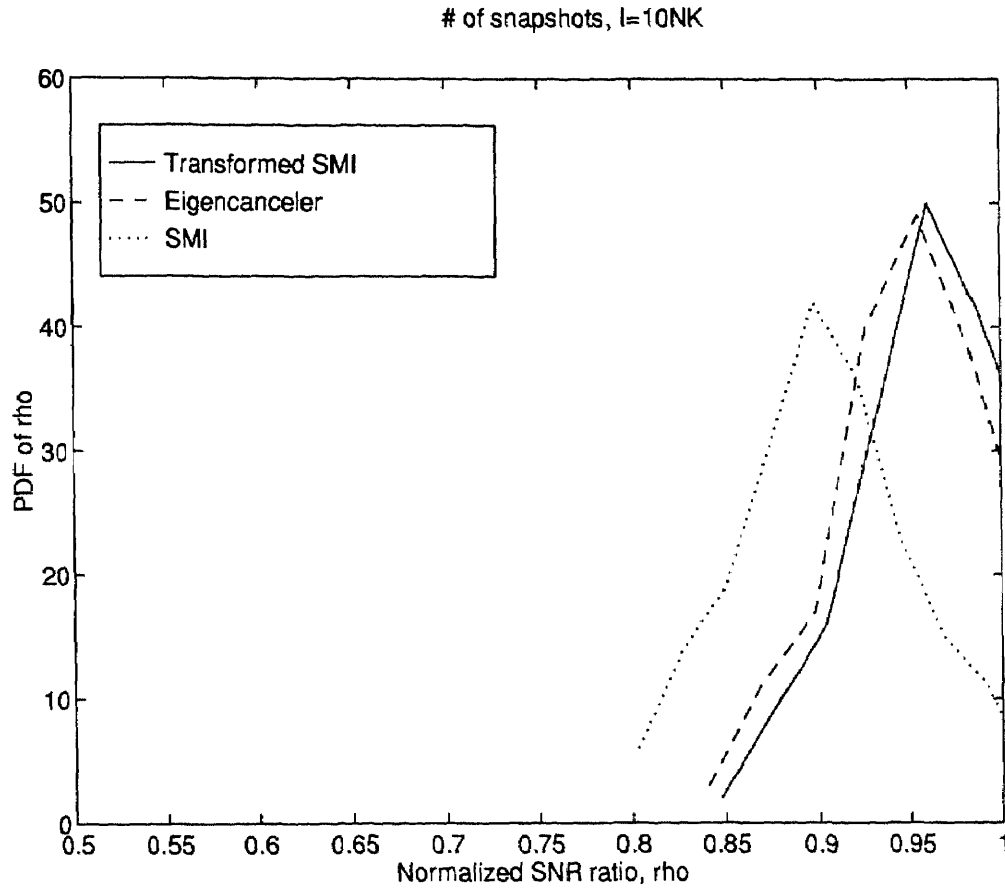
Figure 15: Probability Density Function of ρ, (I = 10NK)
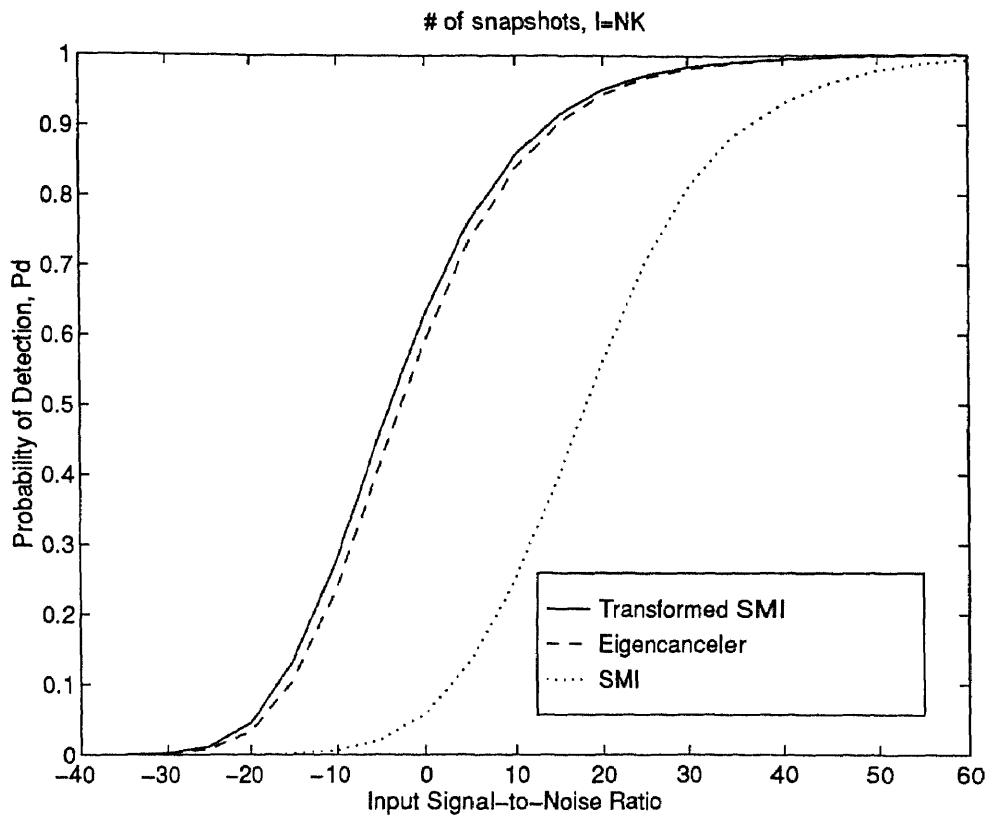
Figure 16: Probability of Detection, P_D (I = NK)
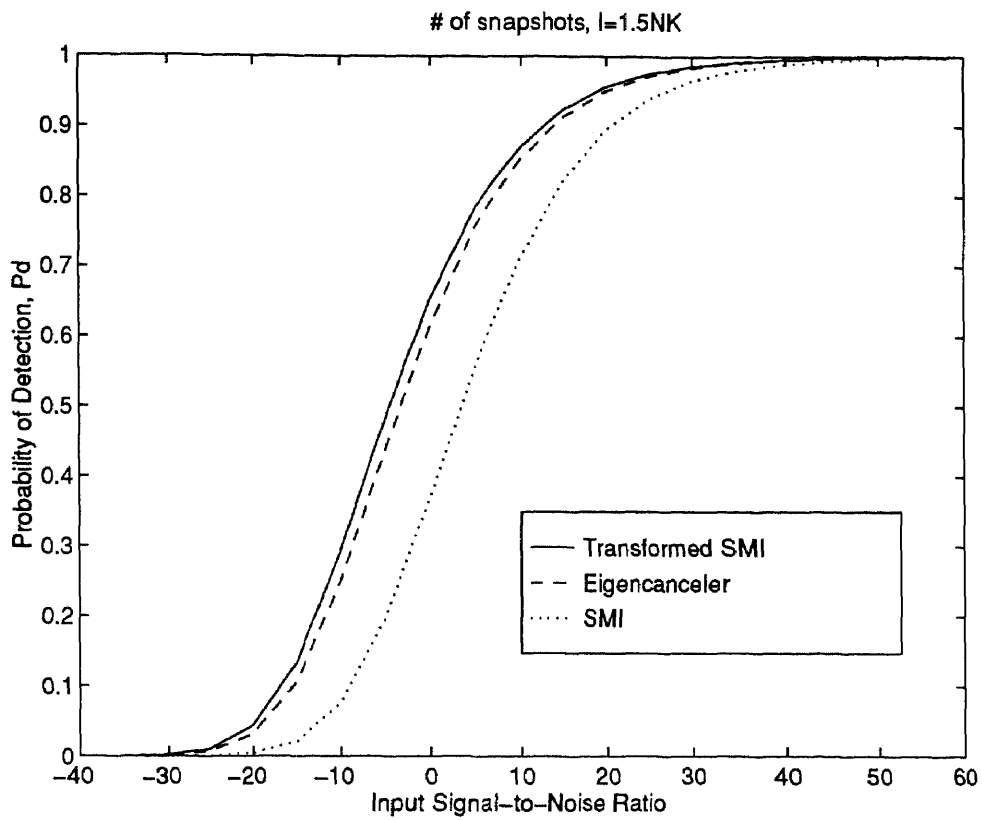
Figure 17: Probability of Detection, P_D (I = 1.5NK)
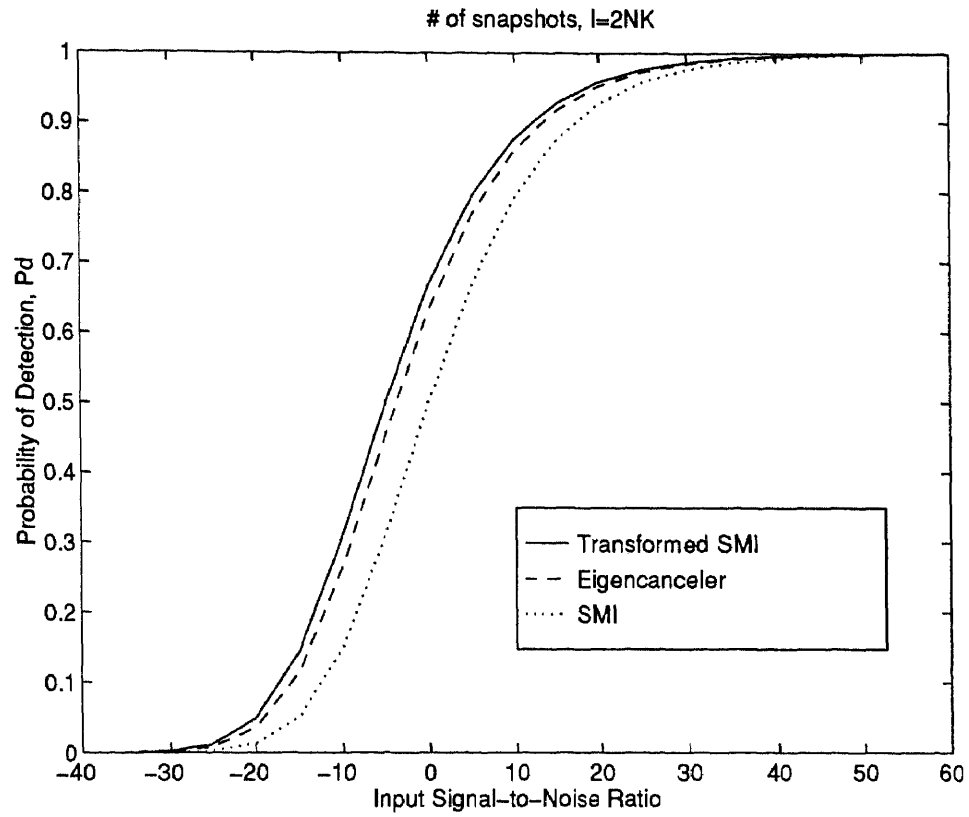
Figure 18: Probability of Detection, P_D ($I = 2NK$)
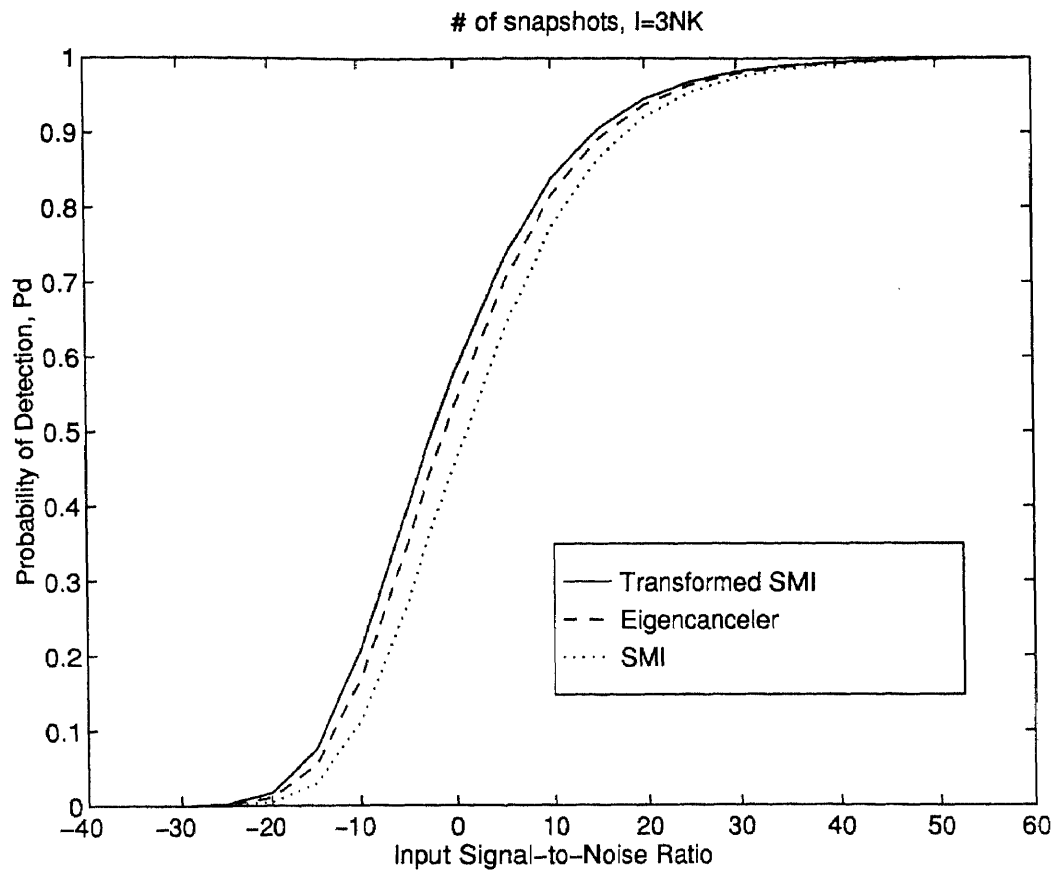
Figure 19: Probability of Detection, P_D (I = 3NK)
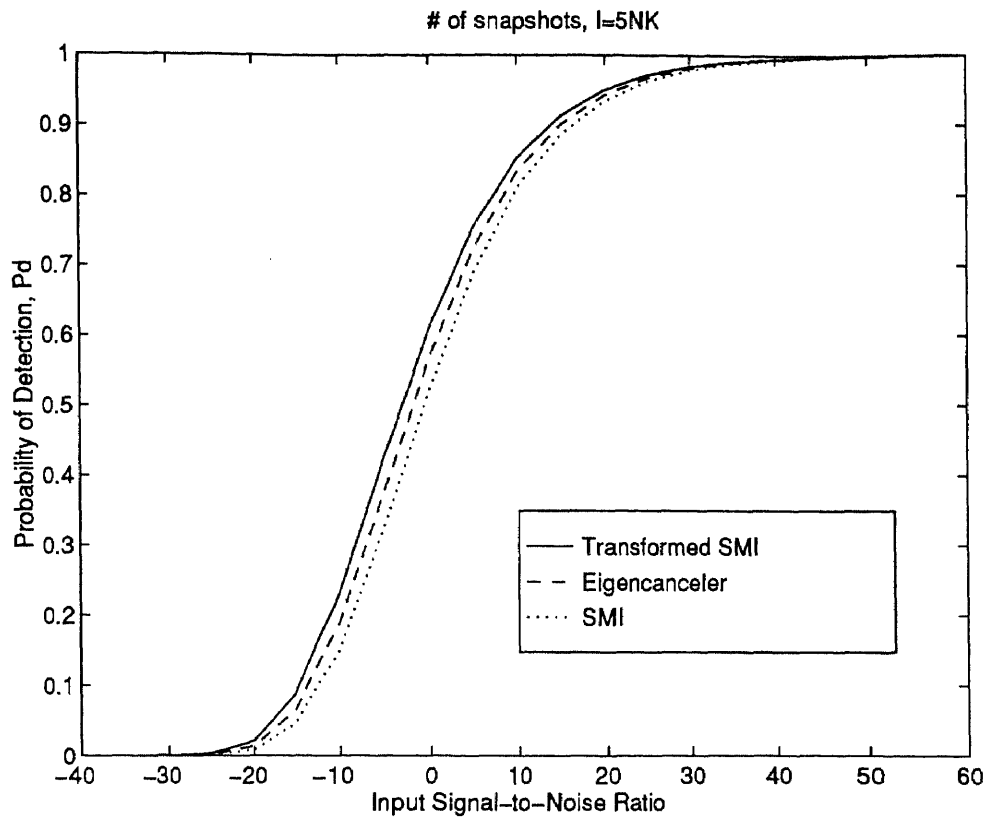
Figure 20: Probability of Detection, P$_D$ (I = 5NK)

# of snapshots, I=10NK
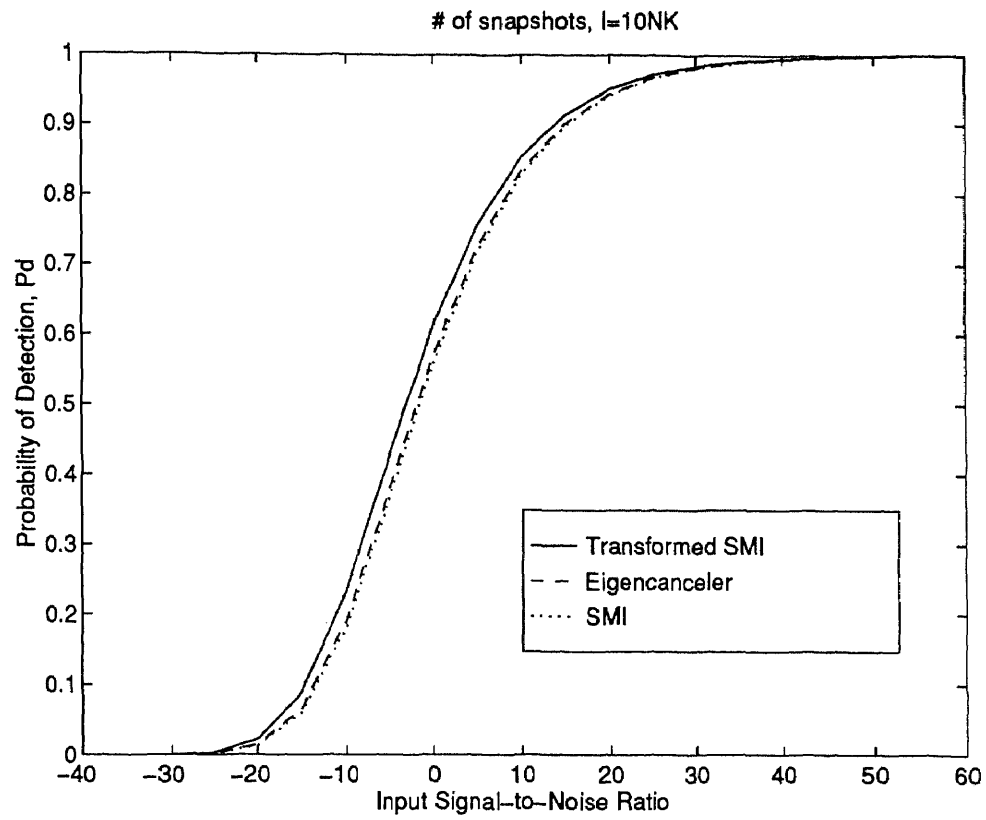
Figure 21: Probability of Detection, P_D (I = 10NK)
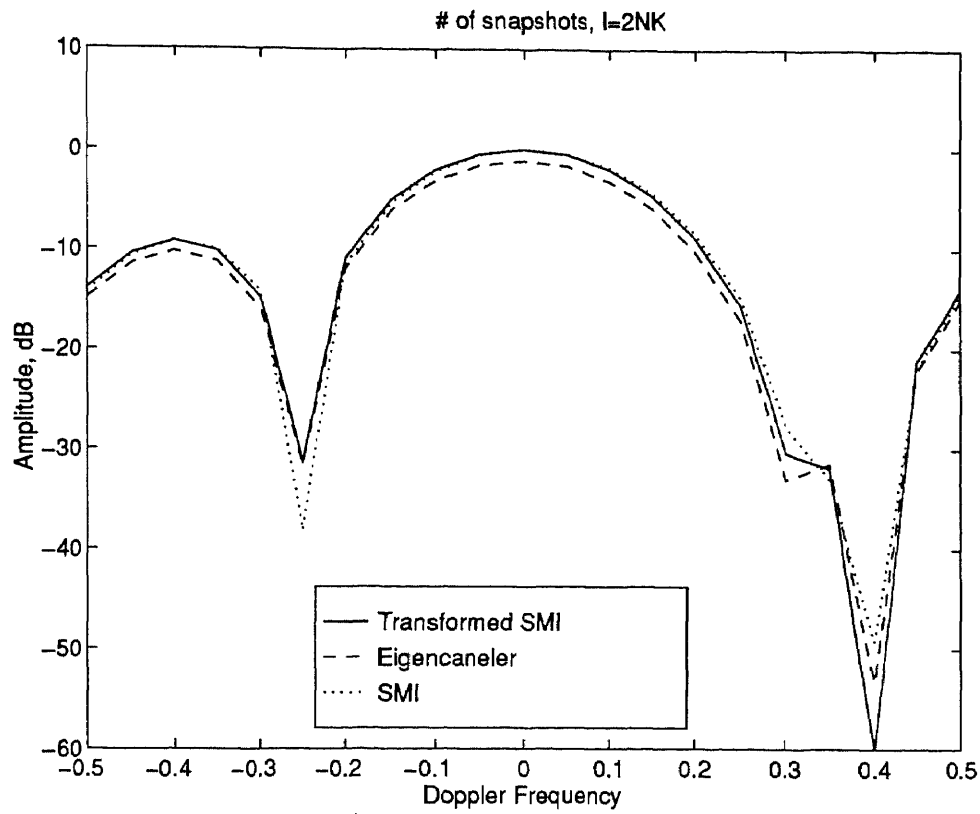
Figure 22: Frequency Pattern (I = 2NK)
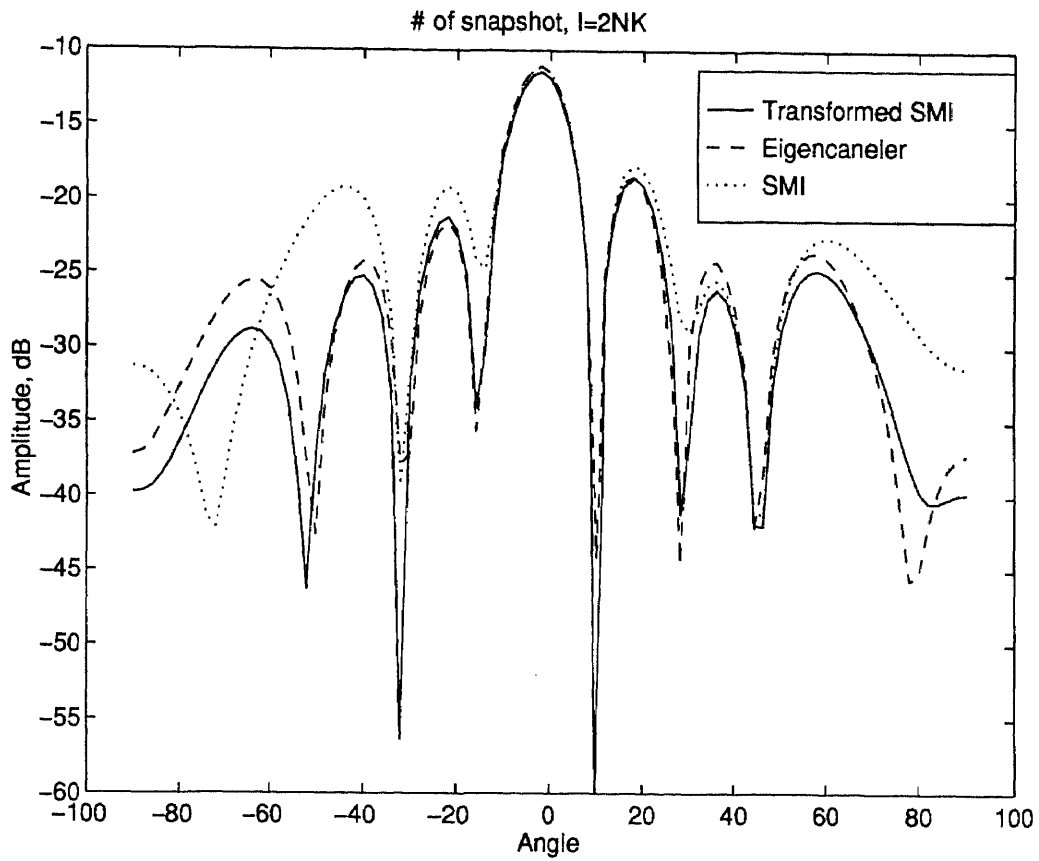
Figure 23: Angle Pattern (I = 2NK)
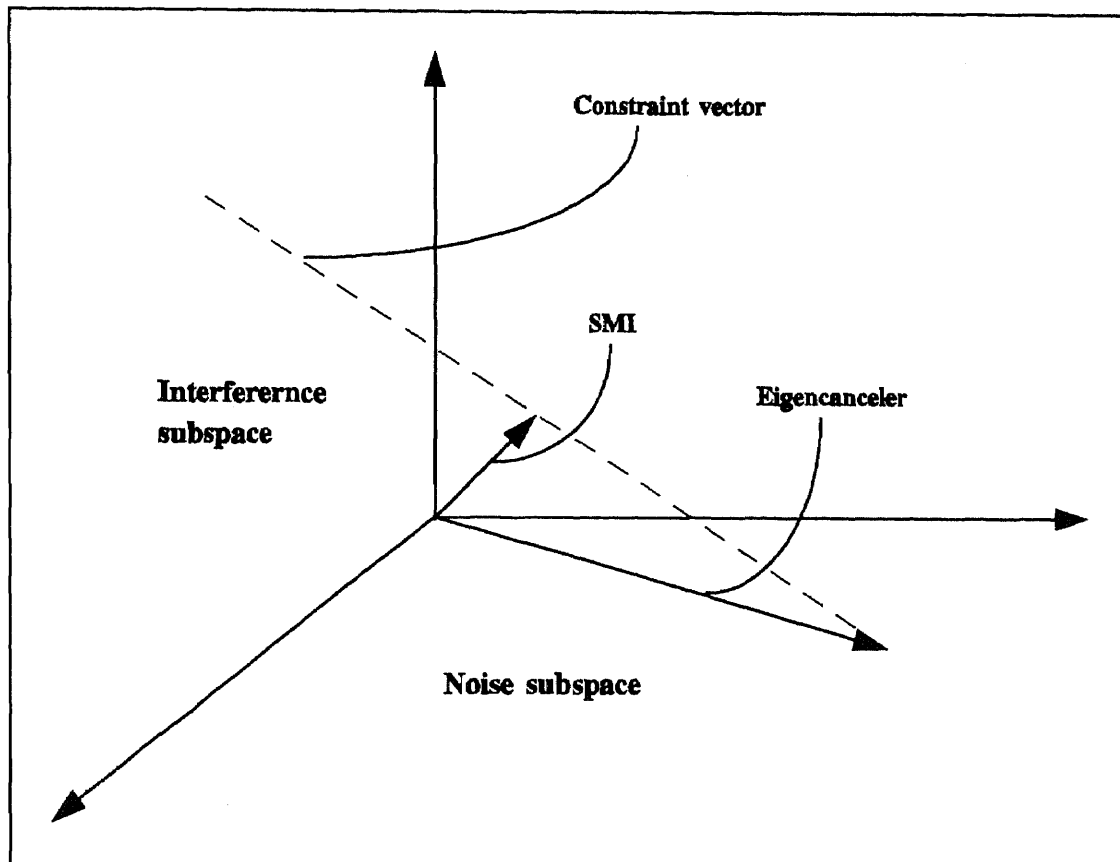
Figure 24: Graphical Representation of Weight Vectors

REFERENCES

[1]   R. A. Monzingo and T. W. Miller, *Introduction to Adaptive Arrays*, Wiley, New York, 1980.

[2]   B. Widrow and S. D. Stearns, *Adaptive Signal Processing*, Prentice Hall, Englewood Cliff, New Jersey, 1985.

[3]   R. T. Compton, Jr., *Adaptive Antennas, Concepts, and Performance*, Prentice Hall, Englewood Cliff, New Jersey, 1989.

[4]   S. Haykin, *Adaptive Filter Theory*, 2nd Edition, Prentice Hall, Englewood Cliff, New Jersey, 1991.

[5]   B. Widrow, et. al., "Adaptive Antenna Systems," Proceedings of IEEE, vol. 55, pp. 2143-2159, December 1967.

[6]   S. P. Applebaum, "Adaptive Arrays," IEEE Transactions on Antennas and Propagation, vol. AP-24, pp. 585-594, September 1976.

[7]   L. E. Brennan, I. S. Reed, "Theory of Adaptive Radar," IEEE Transactions on Aerospace and Electronic Systems, vol. AES-9, NO. 2, pp. 237-252, March 1973.

[8]   I. S. Reed, J. D. Mallett, and L. E. Brennan, "Rapid Convergence Rate in Adaptive Arrays," IEEE Transactions on Aerospace and Electronic Systems, vol. AES-10, NO. 6, pp. 853-863, November 1974.

[9]   E. J. Kelly, "An Adaptive Detection Algorithm," IEEE Transactions on Aerospace and Electronic Systems, vol. AES-22, NO. 1, pp. 115-127, March 1986.

[10] I. P. Kirsteins, D. W. Tufts, "Adaptive Detection Using Low Rank Approximation to a Data Matrix," IEEE Transactions on Aerospace and Electronic Systems, vol. AES-26, NO. 5, pp. 57-67, January 1994.

[11] A. Haimovich, Y. Bar-Ness, "An Eigenanalysis Interference Canceler," IEEE Transactions on Acoustics, Speech, and Signal Processing, vol. ASSP-35, pp. 77-84, January 1991.

[12] E. J. Hendon, I. S. Reed, "A New CFAR Sidelobe Canceler Algorithm for Radar," IEEE Transactions on Aerospace and Electronic Systems, vol. AES-26, NO. 5, pp. 792-803, September 1990.

[13] D. F. Marshall, "A Two step Adaptive Interference Nulling Algorithm for use with Airborne Sensor Arrays," IEEE Proceedings, Seventh SP Workshop on Statistical Signal & Array Processing, pp. 301-304, Quebec City, Canada, June 26-29, 1994.

[14] D. J. Chapman, "Partially Adaptivity for the Large Array," IEEE Transactions on Antennas and Propagation, vol. AP-24, NO. 5, pp. 685-696, September 1976.

[15] B. D. Van Veen, R. A. Roberts, "Partially Adaptive Beamformer Design via output Power Minimization," IEEE Transactions on Acoustics, Speech, and Signal Processing, vol. ASSP-35, NO. 11, pp. 1524-1532, November 1987.

[16] H. Wang, L. Cai, "On Adaptive Multiband Signal Detection with SMI Algorithm," IEEE Transactions on Aerospace and Electronic Systems, vol. AES-26, NO. 5, pp. 768-773, September 1990.

[17] H. Wang, L. Cai, "On Adaptive Multiband Signal Detection with GLR Algorithm," IEEE Transactions on Aerospace and Electronic Systems, vol. AES-27, NO. 2, pp. 225-232, March 1991.

[18] H. Wang, L. Cai, "On Adaptive Spatial-Temporal Processing for Airborne Surveillance Radar Systems," IEEE Transactions on Aerospace and Electronic Systems, vol. AES-30, NO. 3, pp. 660-669, July 1994.

[19] H. Wang, L. Cai, "A Localized Adaptive MTD Processor," IEEE Transactions on Aerospace and Electronic Systems, vol. AES-27 , NO. 3, pp. 532-539, May 1991.

[20] L. E. Brennan, J. D. Mallett, and I. S. Reed, "Adaptive Arrays in Airborne MTI Radar," IEEE Transactions on Antennas and Propagation, vol. AP-24, NO. 5, pp. 607-615, September 1976.

[21] L. Chang, Chien-Chung Yeh, "Performance of DMI and Eigenspace-based Beamformers," IEEE Transactions on Antennas and Propagation, vol. AP-40, NO. 11, pp. 1336-1347, November 1992.

[22] L. Cai, H. Wang, "Performance Comparison of Modified SMI and GLR Algorithms," IEEE Transactions on Aerospace and Electronic Systems, vol. AES-27, NO. 3, pp. 487-491, May 1991.

[23] B. D. Van Veen, "Adaptive Convergence of Linearly Constrained Beamformers Based on Sample Covariance Matrix," IEEE Transactions on Signal Processing, vol. SP-39, NO. 6, pp. 1470-1473, June 1991.

[24]   J. L. Krolik, D. N. Swingler, "On the Mean-Square Error Performance of Adaptive Minimum Variance Beamformers based on Sample Covariance Matrix," IEEE Transactions on Signal Processing, vol. SP-42, NO. 2, pp. 445-448, February 1994.

[25]   B. D. Van Veen, "An Analysis of Several Partially Adaptive Beamformer Designs," IEEE Transactions on Acoustics, Speech, and Signal Processing, vol. ASSP-37, NO. 2, pp. 192-203, February 1989.

[26]   R. Klemm, "Adaptive Clutter Suppression for Airborne Phased Array Radars," IEE Proceedings, vol. 130, Pts. F and H, pp. 125-132, February 1983.

[27]   K. M. Buckley, "Spatial/Spectral Filtering with Linearly Constrained Minimum Variance Beamformers," IEEE Transactions on Acoustics, Speech, and Signal Processing, vol. ASSP-35, pp. 249-266, March 1987.

[28]   R. Nitzberg, "Detection Loss of the Sample Covariance Matrix Inversion Technique," IEEE Transactions on Aerospace and Electronic Systems, vol. AES-20, NO. 6, pp. 824-827, November 1984.

[29]   C. G. Khatri, C. Radhakrishna Rao, "Effects of Estimated Noise Covariance Matrix in Optimal Signal Detection," IEEE Transactions on Acoustics, Speech, and Signal Processing, vol. ASSP-35, NO. 5, pp. 671-679, May 1987.